Exact exchange in relativistic spin-density-functional theory: Exchange splitting versus spin-orbit coupling

E. Engel
Center for Scientific Computing, J.W. Goethe-Universität Frankfurt, Max-von-Laue-Strasse 1, D-60438 Frankfurt/Main, Germany

D. Ködderitzsch and H. Ebert
Department Chemie und Biochemie, Physikalische Chemie, Ludwig-Maximilians-Universität München, Butenandtstrasse 11, D-81377 München, Germany

(Received 26 September 2008; published 30 December 2008)

Recently, the concept of the exact orbital-dependent exchange was introduced into relativistic spin-density-functional theory (RSDFT) within the collinear limit [D. Ködderitzsch *et al.*, Phys. Rev. B **77**, 045101 (2008)]. In this contribution we further expand this exact exchange (EXX) formalism by (i) extending the basic equations to the general noncollinear form of RSDFT and (ii) discussing in detail the solution of the coupled integral equations resulting from orbital-dependent functionals in the framework of RSDFT. The EXX scheme is then applied to open-shell atoms in order to study (i) the relative importance of exchange splitting and spin-orbit coupling, (ii) the consequences of the exact exchange for atomic hyperfine constants, and (iii) the relative stability of the $3d^{n-1}4s^2$ and $3d^n4s^1$ configurations in case of the $3d$ transition-metal elements. In particular, it is demonstrated that the exact exchange, when combined with the orbital-dependent random-phase approximation for correlation, yields s-d-transfer energies which are clearly superior to the values obtained with conventional density functionals.

DOI: 10.1103/PhysRevB.78.235123 PACS number(s): 71.15.Mb, 31.15.E−, 31.30.J−, 32.10.Fn

I. INTRODUCTION AND SUMMARY OF RESULTS

Density functional calculations for magnetic systems are usually based on nonrelativistic spin-density-functional theory (SDFT) (Ref. 1) or extensions including a current dependence[2,3] (for recent applications see, e.g., Refs. 4–6). In practice SDFT is often combined with relativistic density-functional theory (RDFT) (Ref. 7) (for an overview see Ref. 8): as spin-orbit coupling cannot be completely neglected for many interesting magnetic materials, nonrelativistic spin-density functionals for the exchange-correlation (xc) energy E_{xc} are frequently utilized together with the Dirac-type Kohn-Sham (KS) equations of RDFT.

This approach has been given a formal justification a long time ago.[9,10] In its most general form this RDFT approach relies on the density n, the magnetization density $\boldsymbol{m}$, and the paramagnetic current density $\boldsymbol{j}_p$, which emerges as a consequence of the Gordon decomposition of the physical current of RDFT plus an independent coupling of $\boldsymbol{m}$ and $\boldsymbol{j}_p$ to the magnetic field. However, the formulation of xc functionals depending on n, $\boldsymbol{m}$, and $\boldsymbol{j}_p$ simultaneously turned out to be difficult, as the homogeneous electron gas does not lend itself as the starting point for the derivation of approximations. For this reason the $\boldsymbol{j}_p$-dependence of E_{xc} is usually ignored. In the following, we will, for brevity, refer to this reduced RDFT framework as relativistic spin-density-functional theory (RSDFT) in spite of the fact that its fundamental variables are the density n and the magnetization density $\boldsymbol{m}$.

Unfortunately, not even the local-density approximation (LDA) for the associated $E_{\mathrm{xc}}[n,\boldsymbol{m}]$ is available to date, only its exchange-only (x-only) limit is known.[11] In practice, calculations therefore usually exploit RSDFT in the collinear approximation in which $\boldsymbol{m}$ is assumed to have only one component, $\boldsymbol{m}=(0,0,m_z)$. In this limit, one can easily identify relativistic extensions of the spin densities of SDFT, $n_{\pm}=\frac{1}{2}[n(r)\mp m_z(r)/\mu_B]$, and apply nonrelativistic spin-density functionals with these $n_{\pm}$. In addition, the solution of the KS equations of RSDFT was found to be quite involved,[12–17] so that many calculations are based on indirect implementations of RSDFT.

The difficulties with the derivation of suitable $\boldsymbol{m}$ and $\boldsymbol{j}_p$-dependent functionals are automatically resolved, as soon as one allows for orbital-dependent xc functionals as the exact exchange (EXX) E_{x} (for an overview of the concept of implicit xc functionals see Ref. 18). Depending on the formalism in which such functionals are applied, their dependence on the KS spinors ϕ_k translates into a dependence on n, on n plus $\boldsymbol{m}$, or on n plus $\boldsymbol{m}$ plus $\boldsymbol{j}_p$. Orbital-dependent functionals are therefore perfectly suited for use in the framework of R(S)DFT or current-density-functional theory.[4–6]

Orbital-dependent xc functionals and in particular the exact exchange are receiving increasing attention also for quite different reasons. The main point is the fact that the EXX resolves the most prominent problems resulting from the incomplete cancellation of the self-interaction by conventional density functionals as the LDA or the generalized gradient approximation (GGA). As a consequence of the complete elimination of self-interaction one, e.g., obtains a Rydberg series of unoccupied states for neutral atoms,[19] implying the existence of negative atomic ions.[20] Many calculations with the exact exchange also point at an improved description of the band gaps of semiconductors,[21–27] although this conclusion has been questioned recently.[28] Moreover, orbital-dependent correlation functionals can successfully deal with dispersion forces.[29–33]

The concept of orbital-dependent xc functionals has been introduced into RDFT many years ago.[29,34–36] However, only

very recently the EXX scheme was implemented within RSDFT (Ref. 37) (in the following this paper will be referred to as I). In I the basic EXX formalism was presented, restricting the discussion to the collinear limit of RSDFT. In this approach the xc potential and the z component of the xc magnetic field are determined by simultaneous solution of two coupled integral equations in direct extension of the optimized potential method (OPM) (Ref. 19) of nonrelativistic DFT. In addition, the RSDFT analog of the Krieger-Li-Iafrate approximation[38] was derived in order to address the computational inefficiency of EXX calculations on the basis of the full OPM. Some prototype results for atoms were also provided in I, demonstrating the practical feasibility of EXX calculations and making contact to nonrelativistic SDFT.

In the present paper the EXX formalism is expanded and analyzed in more detail (Sec. II). We start with the extension of the concept of orbital-dependent E_{xc} to the general noncollinear form of RSDFT. One finds that in this case four coupled integral equations have to be solved in order to calculate the xc potential $v_{\mathrm{xc}}=\delta E_{\mathrm{xc}}/\delta n$ and the xc magnetic field $\boldsymbol{B}_{\mathrm{xc}}=\delta E_{\mathrm{xc}}/\delta \boldsymbol{m}$. Next we provide all necessary information for the actual solution of the OPM integral equations of collinear RSDFT, in this way completing the formalism introduced in I. In particular, we discuss the construction of orthogonal Green's function G_k of RSDFT, which is the core ingredient of the OPM integral equations. As in the nonrelativistic context,[19] G_k can be expressed in terms of the irregular solutions of the KS equations of RSDFT. Its form, however, turns out to be much more involved due to the intricate structure of the underlying KS equations. On the basis of this representation one can then prove that the exact exchange potential of RSDFT approaches $-1/|\boldsymbol{r}|$ in the asymptotic regime of finite systems.

The formal developments presented here and in paper I also provide a sound basis for the implementation of the exact exchange in standard all-electron schemes for relativistic electronic structure calculations for solids. The construction scheme for G_k directly applies to the tightly bound core states of a solid. A generalization of this scheme to extended band states has recently been used for the discussion of nonmagnetic metals.[39] Its extension to spin-polarized solids is under development. This should allow a comparison with other solid-state OPM approaches in which the spin-orbit coupling of the valence states is taken into account either perturbatively within a Pauli-spinor formalism[40] or indirectly via relativistic pseudopotentials which induce spin-orbit splitting into an otherwise nonrelativistic framework.[41]

In the second part of the paper (Sec. III) we investigate the role of the exact exchange in the case of open-shell atoms. Three topics are addressed: (i) the relative importance of exchange splitting and spin-orbit coupling, (ii) the accuracy of atomic hyperfine constants, and (iii) the relative stability of the $3d^{n-1}4s^2$ and $3d^n4s^1$ configurations of the $3d$ transition-metal elements, i.e., the energy associated with the s-d-transfer process. It is found that, as one might have expected, the spin alignment favored by the exact exchange dominates the KS spectrum over a wider range of Z than observed for conventional density functionals. A prominent example is Pb for which the states of the $6p$ shell are ordered according to good total angular momentum j in case of the LDA and GGA, while this ordering dissolves in the EXX calculation. The modified balance between spin alignment and spin-orbit coupling seems to improve in particular the description of the $4d$ elements: for several of the $4d$ elements the exact exchange provides a much better description of hyperfine constants than the LDA or GGA. Similarly, the EXX scheme yields improved s-d-transfer energies for the $3d$ elements. When combined with an orbital-dependent representation of correlation in the form of the random-phase approximation (RPA),[31,42–44] the resulting s-d-transfer energies closely follow their experimental counterparts throughout the complete $3d$ shell. The maximum deviation is found for Ti, for which the preference for the $3d^24s^2$ configuration is underestimated by 20 mhartree. However, in contrast to the GGA, the orbital-dependent functional clearly predicts the $3d^24s^2$ configuration to be more stable than its $3d^34s^1$ alternative. The agreement between EXX+RPA and experiment is particularly good in the second half of the shell, for which the identification of KS and experimental states is unambiguous. The s-d-transfer energies of the $3d$ elements thus provide another example for the scientific potential of orbital-dependent xc functionals. $\hbar=e=1$ is used throughout this paper. The electron mass is denoted by m_e and not set to 1 in all formulas.

II. THEORY

There exist several approaches to RDFT, differing in the set of fundamental densities exploited for the representation of all relevant functionals (for an overview see Ref. 8). While only the "covariant" form,[7] in which the ground-state four current density $j^\mu=(n,\boldsymbol{j}/c)$ is used, can be given a rigorous foundation in the framework of quantum electrodynamics,[8,45] a second variant turned out to be more useful in practice. This approach[9] relies on the density n and magnetization density $\boldsymbol{m}$ and may be obtained from the four current version of RDFT by use of the Gordon identity and subsequent neglect of the paramagnetic contribution to $\boldsymbol{j}$, so that the dependence on $\boldsymbol{j}$ reduces to a dependence on $\boldsymbol{\nabla}\times\boldsymbol{m}$. Here this latter approach is referred to as RSDFT in spite of the fact that spin is not a good quantum number in RSDFT.

The OPM has been formulated for both the four current version of RDFT (Refs. 29 and 36) and, recently, for the collinear limit of RSDFT,[37] in which $\boldsymbol{m}$ is assumed to have the form $\boldsymbol{m}=(0,0,m_z)$. We will thus start the discussion of the OPM by a generalization of the latter approach to the fully $\boldsymbol{m}$-dependent noncollinear RSDFT formalism.

A. Relativistic spin-density-functional theory: Basics

The Dirac-type KS equations of noncollinear RSDFT are given by[8,9]

$$\{-ic\boldsymbol{\alpha}\cdot\boldsymbol{\nabla}+(\beta-1)m_ec^2+v_{\mathrm{s}}-\mu_B\beta\Sigma\cdot\boldsymbol{B}_{\mathrm{s}}\}\phi_k=\epsilon_k\phi_k, \quad (1)$$

where v_s denotes the standard total KS potential,

$$v_{\mathrm{s}}(\boldsymbol{r})=v_{\mathrm{ext}}(\boldsymbol{r})+v_{\mathrm{H}}(\boldsymbol{r})+v_{\mathrm{xc}}(\boldsymbol{r}), \quad (2)$$

$$v_{\mathrm{H}}(\boldsymbol{r})=\int d^3r'\frac{n(\boldsymbol{r}')}{|\boldsymbol{r}-\boldsymbol{r}'|}, \quad (3)$$

$$v_{\mathrm{xc}}(\boldsymbol{r}) = \frac{\delta E_{\mathrm{xc}}[n,\boldsymbol{m}]}{\delta n(\boldsymbol{r})}, \tag{4}$$

the KS magnetic field $\boldsymbol{B}_s$ is given by

$$\boldsymbol{B}_{\mathrm{s}}(\boldsymbol{r}) = \boldsymbol{B}_{\mathrm{ext}}(\boldsymbol{r}) + \boldsymbol{B}_{\mathrm{xc}}(\boldsymbol{r}), \tag{5}$$

$$\boldsymbol{B}_{\mathrm{xc}}(\boldsymbol{r}) = \frac{\delta E_{\mathrm{xc}}[n,\boldsymbol{m}]}{\delta \boldsymbol{m}(\boldsymbol{r})}, \tag{6}$$

and the density n and magnetization density $\boldsymbol{m}$ are obtained as

$$n(\boldsymbol{r}) = \sum_k \Theta_k |\phi_k(\boldsymbol{r})|^2, \tag{7}$$

$$\boldsymbol{m}(\boldsymbol{r}) = -\mu_B \sum_k \Theta_k \phi_k^\dagger(\boldsymbol{r}) \beta \Sigma \phi_k(\boldsymbol{r}) \qquad \Sigma = \begin{pmatrix} \boldsymbol{\sigma} & 0 \\ 0 & \boldsymbol{\sigma} \end{pmatrix}, \tag{8}$$

$$\Theta_k = \begin{cases} 1 & \text{if } -m_e c^2 < \epsilon_k \leq \epsilon_F \\ 0 & \text{otherwise.} \end{cases} \tag{9}$$

The form of occupation numbers Θ_k implies use of the no-pair approximation, which is applied consistently throughout this work. Moreover, the discussion is restricted to systems without external magnetic field, $\boldsymbol{B}_{\mathrm{ext}}=\boldsymbol{0}$.

The crucial quantity of RSDFT is the xc functional $E_{\mathrm{xc}}[n,\boldsymbol{m}]$. Unfortunately, only the LDA for exchange[11] is available in an explicitly $\boldsymbol{m}$-dependent form, all other inherently relativistic density functionals[46–48] relying on n only.

The situation is much more favorable in case of implicit orbital-dependent functionals as the exact exchange,

$$E_{\mathrm{x}} = -\frac{1}{2} \sum_{k,l} \Theta_k \Theta_l (kl \| lk), \tag{10}$$

$$(ij \| kl) = \int d^3r \int d^3r' \frac{\phi_i^\dagger(\boldsymbol{r}) \phi_k(\boldsymbol{r}) \phi_j^\dagger(\boldsymbol{r}') \phi_l(\boldsymbol{r}')}{|\boldsymbol{r}-\boldsymbol{r}'|}, \tag{11}$$

for which the KS four spinors ϕ_k mediate the density dependence: depending on the framework in which E_{x} is applied, Eq. (10) represents a functional of n, of j^μ or, as in the present situation, of $(n,\boldsymbol{m})$.

The concept of implicit functionals can be directly extended to the relativistic correlation functional E_{c}, for which an exact expression can be derived via standard Green's-function methods.[29] In this case a dependence on all (occupied and unoccupied) ϕ_k and the associated eigenvalues ϵ_k is found.

B. OPM equations of RSDFT: Noncollinear version

Given an orbital-dependent functional as Eq. (10), the obvious first task is the formulation of the OPM equations within the theory at hand (noncollinear RSDFT) in order to determine the associated potential(s) (here v_{xc} and $\boldsymbol{B}_{\mathrm{xc}}$). Using the chain rule for functional differentiation one obtains

$$\frac{\delta E_{\mathrm{xc}}[n,\boldsymbol{m}]}{\delta v_{\mathrm{s}}(\boldsymbol{r})} = \int d^3r' \left\{ \frac{\delta n(\boldsymbol{r}')}{\delta v_{\mathrm{s}}(\boldsymbol{r})} \frac{\delta E_{\mathrm{xc}}}{\delta n(\boldsymbol{r}')} + \frac{\delta \boldsymbol{m}(\boldsymbol{r}')}{\delta v_{\mathrm{s}}(\boldsymbol{r})} \frac{\delta E_{\mathrm{xc}}}{\delta \boldsymbol{m}(\boldsymbol{r}')} \right\}$$
$$= \sum_k \int d^3r' \frac{\delta \phi_k^\dagger(\boldsymbol{r}')}{\delta v_{\mathrm{s}}(\boldsymbol{r})} \frac{\delta E_{\mathrm{xc}}}{\delta \phi_k^\dagger(\boldsymbol{r}')} + \mathrm{c.c.}, \tag{12}$$

$$\frac{\delta E_{\mathrm{xc}}[n,\boldsymbol{m}]}{\delta \boldsymbol{B}_{\mathrm{s}}(\boldsymbol{r})} = \int d^3r' \left\{ \frac{\delta n(\boldsymbol{r}')}{\delta \boldsymbol{B}_{\mathrm{s}}(\boldsymbol{r})} \frac{\delta E_{\mathrm{xc}}}{\delta n(\boldsymbol{r}')} + \frac{\delta \boldsymbol{m}(\boldsymbol{r}')}{\delta \boldsymbol{B}_{\mathrm{s}}(\boldsymbol{r})} \frac{\delta E_{\mathrm{xc}}}{\delta \boldsymbol{m}(\boldsymbol{r}')} \right\}$$
$$= \sum_k \int d^3r' \frac{\delta \phi_k^\dagger(\boldsymbol{r}')}{\delta \boldsymbol{B}_{\mathrm{s}}(\boldsymbol{r})} \frac{\delta E_{\mathrm{xc}}}{\delta \phi_k^\dagger(\boldsymbol{r}')} + \mathrm{c.c.}, \tag{13}$$

where a possible ϵ_k dependence of E_{xc} has been ignored for brevity (its incorporation can follow the scheme of Ref. 29). In order to evaluate the ingredients of Eqs. (12) and (13) one has to determine the variation in the ϕ_k with the basic fields in the KS equations [Eq. (1)]. Following the basic procedure of Ref. 19 one finds

$$\frac{\delta \phi_k(\boldsymbol{r})}{\delta v_{\mathrm{s}}(\boldsymbol{r}')} = -G_k(\boldsymbol{r},\boldsymbol{r}') \phi_k(\boldsymbol{r}'), \tag{14}$$

$$\frac{\delta \phi_k(\boldsymbol{r})}{\delta \boldsymbol{B}_{\mathrm{s}}(\boldsymbol{r}')} = \mu_B G_k(\boldsymbol{r},\boldsymbol{r}') \beta \Sigma \phi_k(\boldsymbol{r}'), \tag{15}$$

with Green's function

$$G_k(\boldsymbol{r},\boldsymbol{r}') = \sum_{l \neq k} \frac{\phi_l(\boldsymbol{r}) \phi_l^\dagger(\boldsymbol{r}')}{\epsilon_l - \epsilon_k}. \tag{16}$$

From Eqs. (7) and (8) one thus obtains for the response functions of RSDFT,

$$\frac{\delta n(\boldsymbol{r}')}{\delta v_{\mathrm{s}}(\boldsymbol{r})} = \chi_{nn}(\boldsymbol{r}',\boldsymbol{r}) = -\sum_k \Theta_k \phi_k^\dagger(\boldsymbol{r}') G_k(\boldsymbol{r}',\boldsymbol{r}) \phi_k(\boldsymbol{r}) + \mathrm{c.c.}, \tag{17}$$

$$\frac{\delta \boldsymbol{m}(\boldsymbol{r}')}{\delta v_{\mathrm{s}}(\boldsymbol{r})} = \chi_{mn}(\boldsymbol{r}',\boldsymbol{r}) = \mu_B \sum_k \Theta_k \phi_k^\dagger(\boldsymbol{r}') \beta \Sigma G_k(\boldsymbol{r}',\boldsymbol{r}) \phi_k(\boldsymbol{r}) + \mathrm{c.c.}, \tag{18}$$

$$\frac{\delta n(\boldsymbol{r}')}{\delta \boldsymbol{B}_{\mathrm{s}}(\boldsymbol{r})} = \chi_{nm}(\boldsymbol{r}',\boldsymbol{r}) = \mu_B \sum_k \Theta_k \phi_k^\dagger(\boldsymbol{r}') G_k(\boldsymbol{r}',\boldsymbol{r}) \beta \Sigma \phi_k(\boldsymbol{r}) + \mathrm{c.c.}, \tag{19}$$

$$\frac{\delta \boldsymbol{m}(\boldsymbol{r}')}{\delta \boldsymbol{B}_{\mathrm{s}}(\boldsymbol{r})} = \chi_{mm}(\boldsymbol{r}',\boldsymbol{r}) = -\mu_B^2 \sum_k \Theta_k \phi_k^\dagger(\boldsymbol{r}') \beta \Sigma G_k(\boldsymbol{r}',\boldsymbol{r}) \beta \Sigma \phi_k(\boldsymbol{r}) + \mathrm{c.c.} \tag{20}$$

[note that $(\beta\Sigma)^\dagger = \Sigma\beta = \beta\Sigma$]. With Eqs. (14), (15), and (17)–(20) one can rewrite Eqs. (12) and (13) as

$$\int d^3r' \{ \chi_{nn}(\boldsymbol{r},\boldsymbol{r}') v_{\mathrm{xc}}(\boldsymbol{r}') + \chi_{nm}(\boldsymbol{r},\boldsymbol{r}') \cdot \boldsymbol{B}_{\mathrm{xc}}(\boldsymbol{r}') \}$$
$$= -\sum_k \int d^3r' \phi_k^\dagger(\boldsymbol{r}) G_k(\boldsymbol{r},\boldsymbol{r}') \frac{\delta E_{\mathrm{xc}}}{\delta \phi_k^\dagger(\boldsymbol{r}')} + \mathrm{c.c.}, \tag{21}$$

$$\int d^3r'\{\chi_{mn}(\mathbf{r},\mathbf{r}')v_{\mathrm{xc}}(\mathbf{r}') + \chi_{mm}(\mathbf{r},\mathbf{r}')\cdot\mathbf{B}_{\mathrm{xc}}(\mathbf{r}')\}$$

$$= \mu_B \sum_k \int d^3r'\,\phi_k^\dagger(\mathbf{r})\beta\Sigma G_k(\mathbf{r},\mathbf{r}')\frac{\delta E_{\mathrm{xc}}}{\delta\phi_k^\dagger(\mathbf{r}')} + \text{c.c.} \quad (22)$$

The collinear limit of the OPM equations [Eqs. (21) and (22)] has been discussed in detail in I to which we refer the interested reader. It can be directly obtained from Eqs. (21) and (22) by dropping those components of χ_{nm}, χ_{mm}, and $\boldsymbol{B}_{\mathrm{xc}}$ which are assumed to be zero in the collinear limit.

C. Relativistic spin-density-functional theory: Atoms

In the simplest description of atoms within RSDFT (Refs. 13 and 14) one assumes $\boldsymbol{m}$ and $\boldsymbol{B}_{\mathrm{xc}}$ to be collinear (noncollinear corrections have been shown to be small[49]) and both v_s and

$$B_{\mathrm{xc}} \equiv -\mu_B B_{\mathrm{xc},z}$$

to be spherical (which implies a suitable spherical averaging procedure). As a direct consequence, the z projection of the total angular momentum, m, is a good quantum number, so that the exact solutions of Eq. (1) may be expanded as

$$\phi_k(\mathbf{r}) = \frac{1}{r}\sum_{lj}\begin{pmatrix} a_k^{ljm}(r)\Omega_{j,l,m}(\Theta,\varphi) \\ ib_k^{ljm}(r)\Omega_{j,2j-l,m}(\Theta,\varphi)\end{pmatrix}, \quad (23)$$

$$\Omega_{jlm} = \sum_{\sigma=\pm 1/2}\sum_{m_l=-l}^{l}\left(lm_l\frac{1}{2}\sigma|jm\right)Y_{lm_l}(\Theta,\varphi)\chi_\sigma, \quad (24)$$

where $(lm_l s\sigma|jm)$ denotes a Clebsch-Gordan coefficient in the definition of Rose.[50] In addition, one can show that the coupling of states with different l is weak,[13] so that l can also serve as a "good" quantum number and only states with different j (but the same m) remain coupled in expansion (23). The specification of the RSDFT-KS equations for open subshell atoms thus basically requires a distinction between states with $2|m|=2l+1$,

$$\phi_{nlm}(\mathbf{r}) = \frac{1}{r}\begin{pmatrix} a_{nlm}(r)\Omega_{l+1/2,l,m}(\Theta,\varphi) \\ ib_{nlm}(r)\Omega_{l+1/2,l+1,m}(\Theta,\varphi)\end{pmatrix}, \quad (25)$$

and states with $2|m|<2l+1$,

$$\phi_{nlm\sigma}(\mathbf{r}) = \frac{1}{r}\sum_{s=\pm 1}\begin{pmatrix} a^s_{nlm\sigma}(r)\Omega_{l+s/2,l,m}(\Theta,\varphi) \\ ib^s_{nlm\sigma}(r)\Omega_{l+s/2,l+s,m}(\Theta,\varphi)\end{pmatrix}. \quad (26)$$

In order to formulate the KS equations for the (real) radial spinors a_{nlm}, b_{nlm}, $a^s_{nlm\sigma}$, and $b^s_{nlm\sigma}$, resulting from insertion of Eqs. (25) and (26) into Eq. (1), it is most convenient to combine all components into a single four component vector,

$$\varphi_k(r) = \begin{pmatrix} a_k^+(r) \\ b_k^+(r) \\ a_k^-(r) \\ b_k^-(r)\end{pmatrix}, \quad (27)$$

with the understanding that $k\equiv nlm\sigma$ in case of $2|m|<2l+1$ and $k\equiv nlm$, $a_k^+=a_k$, $b_k^+=b_k$, and $a_k^-=b_k^-\equiv 0$ for $2|m|=2l+1$. The KS equations can then be written as[17]

$$\{T_l(r) + V_{lm}(r)\}\varphi_k(r) = \epsilon_k\varphi_k(r), \quad (28)$$

with

$$T_l(r) = c\begin{pmatrix} 0 & -\frac{\partial}{\partial r} - \frac{l+1}{r} & 0 & 0 \\ \frac{\partial}{\partial r} - \frac{l+1}{r} & -2m_e c & 0 & 0 \\ 0 & 0 & 0 & -\frac{\partial}{\partial r} + \frac{l}{r} \\ 0 & 0 & \frac{\partial}{\partial r} + \frac{l}{r} & -2m_e c\end{pmatrix}, \quad (29)$$

$$V_{lm}(r) = v_s(r) + \Lambda_{lm}B_{\mathrm{xc}}(r), \quad (30)$$

$$\Lambda_{lm} = \begin{pmatrix} \frac{2m}{2l+1} & 0 & C_{lm} & 0 \\ 0 & \frac{2m}{2l+3} & 0 & 0 \\ C_{lm} & 0 & -\frac{2m}{2l+1} & 0 \\ 0 & 0 & 0 & -\frac{2m}{2l-1}\end{pmatrix}, \quad (31)$$

$$C_{lm} = -\frac{[(2l+1)^2 - (2m)^2]^{1/2}}{2l+1}. \quad (32)$$

The corresponding orthonormality and completeness relations are given by

$$\int_0^\infty dr\varphi^\dagger_{nlm\sigma}(r)\varphi_{n'lm\sigma'}(r) = \delta_{nn'}\delta_{\sigma\sigma'}, \quad (33)$$

$$\sum_{n\sigma}\varphi_{nlm\sigma}(r)\varphi^\dagger_{nlm\sigma}(r') = \delta(r-r'), \quad (34)$$

with obvious reductions for states with $2|m|=2l+1$.

The densities n and m_z are obtained by insertion of Eqs. (25) and (26) into Eqs. (7) and (8) plus subsequent spherical averaging (in order to be consistent with the assumption of spherically symmetric potentials),

$$n(r) = \frac{1}{4\pi r^2}\sum_k \Theta_k\varphi_k^\dagger(r)\varphi_k(r), \quad (35)$$

$$m_z(r) = -\frac{\mu_B}{4\pi r^2}\sum_k \Theta_k \varphi_k^\dagger(r)\Lambda_{lm}\varphi_k(r). \tag{36}$$

The Hartree energy corresponding to the KS states (25) and (26) is obtained as

$$E_{\mathrm{H}} = \frac{1}{2}\sum_{k,l}\Theta_k\Theta_l(kl\,\|\,kl), \tag{37}$$

with the Slater integrals $(kl\|kl)$ given by

$$\begin{aligned}(kl\,\|\,kl) = (-1)^{m+m'+1}\sum_{s_1,s_2,s_1',s_2'=\pm 1}\sum_{L=0}^{\infty}\frac{1+(-1)^L}{2(2L+1)^2}\int_0^\infty dr\int_0^\infty dr'\,\frac{r_<^L}{r_>^{L+1}}[a_{nlm}^{s_1}(r)a_{nlm}^{s_2}(r)+b_{nlm}^{s_1}(r)b_{nlm}^{s_2}(r)]\\ \times[a_{n'l'm'}^{s_1'}(r')a_{n'l'm'}^{s_2'}(r')+b_{n'l'm'}^{s_1'}(r')b_{n'l'm'}^{s_2'}(r')][(2l+s_1+1)(2l+s_2+1)(2l'+s_1'+1)(2l'+s_2'+1)]^{1/2}\\ \times\left(l+\frac{s_1}{2},\frac{1}{2};l+\frac{s_2}{2},-\frac{1}{2}\middle|L,0\right)\left(l+\frac{s_1}{2},-m;l+\frac{s_2}{2},m\middle|L,0\right)\\ \times\left(l'+\frac{s_2'}{2},\frac{1}{2};l'+\frac{s_1'}{2},-\frac{1}{2}\middle|L,0\right)\left(l'+\frac{s_2'}{2},-m';l'+\frac{s_1'}{2},m'\middle|L,0\right)\end{aligned} \tag{38}$$

$[r_>=\max(r,r');r_<=\min(r,r')]$. Note that no spherical averaging is applied at this point—the angular integrations inherent in $(kl\|kl)$ after use of the multipole expansion of the Coulomb interaction are performed without any modification. Only the monopole contribution $(L=0)$ to Slater integral (38) is included in the standard form of E_H and v_H for spherical systems,

$$E_H = \frac{(4\pi)^2}{2}\int_0^\infty r^2dr\int_0^\infty r'^2dr'\frac{n(r)n(r')}{r_>} \;\Leftrightarrow\; v_H(r) = 4\pi\int_0^\infty r'^2dr'\frac{n(r')}{r_>}, \tag{39}$$

with $n(r)$ given by Eq. (35). All other multipoles in Eq. (38) are usually absorbed into the exchange term.[19,51]

It remains to specify exchange energy (10) for the atomic states (25) and (26). In this case the relevant Slater integral reads

$$\begin{aligned}(kl\,\|\,lk) = \sum_{s_1,s_2,s_1',s_2'=\pm 1}\sum_{L=0}^{\infty}\sum_{M=-L}^{L}\delta_{M,m-m'}\frac{1+(-1)^{l+l'+L}}{2(2L+1)^2}\int_0^\infty dr\int_0^\infty dr'\,\frac{r_<^L}{r_>^{L+1}}[a_{nlm}^{s_1}(r)a_{n'l'm'}^{s_1'}(r)+b_{nlm}^{s_1}(r)b_{n'l'm'}^{s_1'}(r)]\\ \times[a_{n'l'm'}^{s_2'}(r')a_{nlm}^{s_2}(r')+b_{n'l'm'}^{s_2'}(r')b_{nlm}^{s_2}(r')][(2l+s_1+1)(2l'+s_1'+1)(2l+s_2+1)(2l'+s_2'+1)]^{1/2}\\ \times\left(l+\frac{s_1}{2},\frac{1}{2};l'+\frac{s_1'}{2},-\frac{1}{2}\middle|L,0\right)\left(l+\frac{s_1}{2},-m;l'+\frac{s_1'}{2},m'\middle|L,m'-m\right)\\ \times\left(l+\frac{s_2}{2},\frac{1}{2};l'+\frac{s_2'}{2},-\frac{1}{2}\middle|L,0\right)\left(l+\frac{s_2}{2},-m;l'+\frac{s_2'}{2},m'\middle|L,m'-m\right),\end{aligned} \tag{40}$$

with $a_{nlm}^-=b_{nlm}^-=0$ for states with $2|m|=2l+1$.

D. OPM equations of RSDFT: Spherical version

The simplest way to derive the radial OPM integral equations for the spherically symmetric system introduced in Sec. II C is to consider the xc energy as an implicit functional of spherical densities (35) and (36), i.e., for E_{xc} being an explicit functional of the radial spinors [Eq. (27)] only. Moreover, it turns out to be more convenient to formulate the OPM in terms of the relativistic spin densities,

$$n_\pm(r) = \frac{1}{2}\left[n(r) \mp \frac{m_z(r)}{\mu_B}\right] = \sum_k \Theta_k\varphi_k^\dagger(r)P_\pm\varphi_k(r), \tag{41}$$

with the projection operators

$$P_\pm = \frac{1}{2}[1 \pm \Lambda_{lm}]. \tag{42}$$

The associated spin-dependent potentials are given by

$$v_{\mathrm{xc},\pm}(r) = v_{\mathrm{xc}}(r) \pm B_{\mathrm{xc}}(r), \tag{43}$$

$$v_{\mathrm{s},\pm}(r) = v_{\mathrm{ext}}(r) + v_{\mathrm{H}}(r) + v_{\mathrm{xc},\pm}(r) \Leftrightarrow V_{lm}(r) = \sum_{\sigma=\pm} P_\sigma v_{\mathrm{s},\sigma}(r). \tag{44}$$

As discussed in Sec. II B the chain rule for functional differentiation is applied to obtain

$$\frac{\delta E_{\mathrm{xc}}[n_+,n_-]}{\delta v_{\mathrm{s},\sigma}(r)} = \sum_{\sigma'=\pm} \int_0^\infty dr' \frac{\delta[4\pi r'^2 n_{\sigma'}(r')]}{\delta v_{\mathrm{s},\sigma}(r)} \frac{\delta E_{\mathrm{xc}}}{\delta[4\pi r'^2 n_{\sigma'}(r')]}$$

$$= \sum_k \int_0^\infty dr' \frac{\delta\varphi_k(r')}{\delta v_{\mathrm{s},\sigma}(r)} \frac{\delta E_{\mathrm{xc}}}{\delta\varphi_k(r')}. \tag{45}$$

The crucial ingredient of Eq. (45), $\delta\varphi_k/\delta v_{s,\sigma}$, is derived by variation in the potentials in Eq. (28) using Eq. (44). One obtains

$$\frac{\delta\varphi_k(r)}{\delta v_{\mathrm{s},\sigma}(r')} = -G_k(r,r')P_\sigma\varphi_k(r'), \tag{46}$$

with Green's function G_k satisfying

$$\{\vec{T}_l(r) + V_{lm}(r) - \epsilon_k\}G_k(r,r') = \delta(r-r') - \varphi_k(r)\varphi_k^\dagger(r'). \tag{47}$$

The formal solution of Eq. (47) is given by

$$G_{nlm\sigma}(r,r') = \sum_{n'\sigma'\neq n\sigma} \frac{\varphi_{n'lm\sigma'}(r)\varphi^\dagger_{n'lm\sigma'}(r')}{\epsilon_{n'lm\sigma'} - \epsilon_{nlm\sigma}}, \tag{48}$$

with the symmetry

$$G_k^\dagger(r,r') = G_k(r',r). \tag{49}$$

From Eq. (46) one finds for the variation in the densities [Eq. (41)] with the potentials

$$\frac{\delta[4\pi r^2 n_\sigma(r)]}{\delta v_{\mathrm{s},\sigma'}(r')} = \chi_{\sigma\sigma'}(r,r')$$

$$= -2\sum_k \Theta_k\varphi_k^\dagger(r)P_\sigma G_k(r,r')P_{\sigma'}\varphi_k(r'), \tag{50}$$

where it has been used that φ_k, G_k, and Λ_{lm} are real. Defining

$$Q_\sigma(r) = -\sum_k \int_0^\infty dr' \varphi_k^\dagger(r)P_\sigma G_k(r,r')\frac{\delta E_{\mathrm{xc}}}{\delta\varphi_k(r')}, \tag{51}$$

one finally arrives at the coupled radial OPM equations for spherical systems,

$$\sum_{\sigma=\pm}\int_0^\infty dr'\chi_{+\sigma}(r,r')v_{\mathrm{xc},\sigma}(r') = Q_+(r), \tag{52}$$

$$\sum_{\sigma=\pm}\int_0^\infty dr'\chi_{-\sigma}(r,r')v_{\mathrm{xc},\sigma}(r') = Q_-(r). \tag{53}$$

As in the general noncollinear case, a possible ϵ_k dependence of E_{xc} has been suppressed in the present derivation. It can, however, be included straightforwardly, in close analogy to Ref. 29. The next step toward the solution of Eqs. (52) and (53) is an analysis of Green's function G_k.

E. OPM equations of RSDFT: Radial Green's function

In the case of spherical systems the evaluation of Green's function G_k needs not rely on Eq. (48), which requires the calculation of all occupied and unoccupied KS states. Rather one can resort to a direct solution of the differential equation [Eq. (47)]. For the two component states with $|2m|=2l+1$ this solution can closely follow the scheme introduced in Refs. 29 and 34. Its analog for the states with $|2m|<2l+1$ is somewhat more tricky and therefore discussed in this section.

One first notes that Eq. (48) together with the orthonormality of the radial spinors [Eq. (33)] leads to

$$\int_0^\infty dr' G_k(r,r')\varphi_k(r') = 0. \tag{54}$$

Next one introduces the additional non-normalizable solutions of the KS equations [Eq. (28)] for given eigenvalue ϵ_k. In case of states with $|2m|<2l+1$ one has four linearly independent solutions $\chi_{k;j}$,

$$\{T_l(r) + V_{lm}(r) - \epsilon_k\}\chi_{k;j}(r) = 0, \quad j = 1,2,3,4. \tag{55}$$

The physically interesting normalizable solution φ_k will be identified with $\chi_{k;1}$. The other three solutions will be characterized in more detail later. For the moment only their linear independence is of relevance. At this point it is most convenient to drop the index k for the state, as the following analysis applies to each state separately. For any pair of the χ_j (for the same state k) one can easily show that

$$\partial_r[\chi_i^\dagger(r)i\Sigma_2\chi_j(r)] = 0 \quad \forall\, i,j. \tag{56}$$

Equation (56) allows for the normalization

$$\chi_i^\dagger(r)i\Sigma_2\chi_j(r) = \lambda_{ij} \quad (\lambda_{ij} = -\lambda_{ji}), \tag{57}$$

with the constants λ_{ij} still to be determined.

In order to construct G_k one next sets up the fundamental matrix F corresponding to the radial KS equations [Eq. (27)], i.e., a system of four coupled linear differential equations of first order.[52] Taking into account the difference in ordering between the set of equations [Eq. (28)] and standard textbook results, the fundamental matrix reads

$$F = \begin{pmatrix} -\chi_{2,1} & -\chi_{2,2} & -\chi_{2,3} & -\chi_{2,4} \\ \chi_{1,1} & \chi_{1,2} & \chi_{1,3} & \chi_{1,4} \\ -\chi_{4,1} & -\chi_{4,2} & -\chi_{4,3} & -\chi_{4,4} \\ \chi_{3,1} & \chi_{3,2} & \chi_{3,3} & \chi_{3,4} \end{pmatrix}, \tag{58}$$

with the understanding that $\chi_{i,j}$ is the ith component of the jth solution of the eigenvalue problem with eigenvalue ϵ_k. The determinant of the fundamental matrix is a constant as the trace of the coefficient matrix of the set of linear differential equations [Eq. (28)] vanishes. The precise value of the determinant must be consistent with the pair conditions (57). Using Eq. (57) to eliminate either components 3 and 4 or, alternatively, components 1 and 2 of all solutions, one obtains after combination of the two results

$$\det(F) = \lambda_{12}\lambda_{34} + \lambda_{13}\lambda_{42} + \lambda_{14}\lambda_{23}, \tag{59}$$

which illustrates the relation between the conserved pair products [Eq. (57)] and the Wronski determinant.

The core quantity of Green's function is the product of the fundamental matrix and its inverse, $F(r)F^{-1}(r')$. The inverse fundamental matrix may be formalized as

$$F_{ij}^{-1}(r) = \frac{1}{\det(F)} \sum_{n \neq i} \bar{\lambda}_{in} \chi_{jn}(r) \tag{60}$$

with the $\bar{\lambda}_{ik}$ given by

$$\bar{\lambda}_{12} = \lambda_{34}, \quad \bar{\lambda}_{13} = \lambda_{42}, \quad \bar{\lambda}_{14} = \lambda_{23},$$

$$\bar{\lambda}_{23} = \lambda_{14}, \quad \bar{\lambda}_{24} = \lambda_{31}, \quad \bar{\lambda}_{34} = \lambda_{12}. \tag{61}$$

By construction one has

$$i\Sigma_2 = i\Sigma_2 F(r) F^{-1}(r) = \frac{1}{\det(F)} \sum_i \chi_i(r) \sum_{j \neq i} \bar{\lambda}_{ij} \chi_j^\dagger(r). \tag{62}$$

The product of the fundamental matrix and its inverse at different r values allows to set up Green's function. With the overall normalization

$$\det(F) = \frac{1}{c^2}, \tag{63}$$

the function

$$\Gamma(r,r') = c \sum_{i<j} \{\Theta(r-r') \chi_i(r) \bar{\lambda}_{ij} \chi_j^\dagger(r') + \Theta(r'-r) \chi_j(r) \bar{\lambda}_{ij} \chi_i^\dagger(r')\} \tag{64}$$

can be shown to satisfy

$$\{\vec{T}_l(r) + V_{lm}(r) - \epsilon\} \Gamma(r,r') = \delta(r-r') \tag{65}$$

and

$$\Gamma^\dagger(r',r) = \Gamma(r,r'). \tag{66}$$

In terms of $\Gamma(r,r')$ one can finally express Green's function (48) as

$$G(r,r') = \Gamma(r,r') + C\varphi(r)\varphi^\dagger(r') - \int_0^\infty dr'' \Gamma(r,r'')\varphi(r'')\varphi^\dagger(r') - \int_0^\infty dr'' \varphi(r)\varphi^\dagger(r'')\Gamma(r'',r'), \tag{67}$$

$$C = \int_0^\infty dr \int_0^\infty dr' \varphi^\dagger(r) \Gamma(r,r') \varphi(r'). \tag{68}$$

On the basis of Eqs. (65) and (66) one can explicitly verify that Green's function (67) satisfies the differential equation [Eq. (47)] and the boundary condition [Eq. (54)]. Note that the existence of form (67) requires all those $\bar{\lambda}_{ij}$ (with $i<j$) to vanish for which

$$\int_r^\infty dr' \chi_i^\dagger(r') \varphi(r')$$

does not exist.

This constraint as well as normalization (63) have to be taken into account when choosing the coefficients λ_{ij}. The simplest choice, which simultaneously reflects the general symmetry of the problem, is

$$\lambda_{12} = \lambda_{34} = \frac{1}{c}, \tag{69}$$

$$\lambda_{13} = \lambda_{42} = \lambda_{14} = \lambda_{23} = 0, \tag{70}$$

so that

$$\bar{\lambda}_{ij} = \lambda_{ij}, \tag{71}$$

$$\bar{\lambda} = \lambda = \frac{1}{c} i\Sigma_2, \tag{72}$$

and thus

$$\Gamma(r,r') = \Theta(r-r')[\chi_1(r)\chi_2^\dagger(r') + \chi_3(r)\chi_4^\dagger(r')] + \Theta(r'-r)[\chi_2(r)\chi_1^\dagger(r') + \chi_4(r)\chi_3^\dagger(r')]. \tag{73}$$

It remains to construct the non-normalizable solutions χ_2, χ_3, and χ_4 in accordance with Eqs. (69) and (70). The linearly independent solutions of Eq. (55) are most conveniently characterized in terms of the boundary conditions for small and large r values. Detailed analysis of Eq. (55) yields the following elementary solutions for small r (to leading order):

$$\chi_A = r^g \begin{pmatrix} 1 \\ \frac{v_{-1}}{(g+l+1)} \\ 0 \\ 0 \end{pmatrix} \chi_A^{(0)} + \cdots, \tag{74}$$

$$\chi_B = r^{-g} \begin{pmatrix} \frac{v_{-1}}{(g+l+1)} \\ 1 \\ 0 \\ 0 \end{pmatrix} \chi_B^{(0)} + \cdots, \tag{75}$$

$$\chi_C = r^{-f} \begin{pmatrix} 0 \\ 0 \\ 1 \\ -\frac{v_{-1}}{(f+l)} \end{pmatrix} \chi_C^{(0)} + \cdots, \tag{76}$$

$$\chi_D = r^{f} \begin{pmatrix} 0 \\ 0 \\ -\frac{v_{-1}}{(f+l)} \\ 1 \end{pmatrix} \chi_D^{(0)} + \cdots, \tag{77}$$

with $v_{-1} = -Z/c$,

$$g = [(l+1)^2 - v_{-1}^2]^{1/2}, \tag{78}$$

$$f = [l^2 - v_{-1}^2]^{1/2}, \tag{79}$$

and $\chi_{A-D}^{(0)}$ being constants to be determined by normalization. One can verify directly that Eq. (57) holds for any pair of these solutions. Note that in practice higher order corrections stabilize the numerical treatment. Without giving any details, we furthermore remark that for finite nuclear charge distributions also logarithmic terms become relevant.

The discussion of the asymptotic solutions for large r depends quite sensitively on the asymptotic form of the KS potentials,

$$v_s(r) = \frac{v_1}{r} + \frac{v_2}{r^2} + \cdots, \tag{80}$$

$$B_{\mathrm{xc}}(r) = B_0 + \frac{B_1}{r} + \frac{B_2}{r^2} + \cdots. \tag{81}$$

It turns out (see below) that the case $B_0 = B_1 = 0$ is relevant in the present situation. In this case one finds as elementary solutions for large r,

$$\bar{\chi}_A = r^{\alpha} e^{-\beta r} \begin{pmatrix} 1 \\ \frac{\epsilon}{\beta c} \\ 0 \\ 0 \end{pmatrix} \bar{\chi}_A^{(0)} + \cdots, \tag{82}$$

$$\bar{\chi}_B = r^{-\alpha} e^{\beta r} \begin{pmatrix} 1 \\ \frac{-\epsilon}{\beta c} \\ 0 \\ 0 \end{pmatrix} \bar{\chi}_B^{(0)} + \cdots, \tag{83}$$

$$\bar{\chi}_C = r^{\alpha} e^{-\beta r} \begin{pmatrix} 0 \\ 0 \\ 1 \\ \frac{\epsilon}{\beta c} \end{pmatrix} \bar{\chi}_C^{(0)} + \cdots, \tag{84}$$

$$\bar{\chi}_D = r^{-\alpha} e^{\beta r} \begin{pmatrix} 0 \\ 0 \\ 1 \\ \frac{-\epsilon}{\beta c} \end{pmatrix} \bar{\chi}_D^{(0)} + \cdots, \tag{85}$$

with

$$\alpha = -\frac{(m_e + \epsilon/c^2)v_1}{\beta}, \tag{86}$$

$$\beta = [-\epsilon(2m_e + \epsilon/c^2)]^{1/2}. \tag{87}$$

Again Eq. (57) is satisfied for any pair of the $\bar{\chi}_j$.

The normalizable solution $\varphi = \chi_1$ is obtained by combination of the elementary solutions χ_A and χ_D at the origin and $\bar{\chi}_A$ and $\bar{\chi}_C$ for large r.[17] If integrated outward individually, both χ_A and χ_D lead to solutions which diverge for $r \to \infty$, at least as long as $c \neq \infty$. Only the combination of χ_A and χ_D decays exponentially. Analogously, if $\bar{\chi}_A$ and $\bar{\chi}_C$ are integrated inward individually, the results diverge at the origin, provided that $c \neq \infty$. In other words, all χ_{A-D} and $\bar{\chi}_{A-D}$ individually are linearly independent of φ as long as $c \neq \infty$. One can thus choose

$$\chi_1 = \varphi, \tag{88}$$

$$\chi_3 = \begin{cases} \bar{\chi}_C & \text{if } \bar{\chi}_A \text{ dominates in } \varphi \\ \bar{\chi}_A & \text{if } \bar{\chi}_C \text{ dominates in } \varphi, \end{cases} \tag{89}$$

$$\chi_4 = \begin{cases} \chi_D & \text{if } \chi_A \text{ dominates in } \varphi \\ \chi_A & \text{if } \chi_D \text{ dominates in } \varphi. \end{cases} \tag{90}$$

Finally, χ_2 is chosen so that Eq. (57) is satisfied at the outermost extremum of φ, following the basic strategy of Ref. 19. The solution resulting from inward and outward integrations starting at this point is then irregular both for $r \to 0$ and for $r \to \infty$.

For $c \to \infty$ this scheme can no longer be used as one finds two fully regular solutions, reflecting the fact that orbital (26) has to become an eigenstate of the spin operator. In this limit, one can combine each of the two regular solutions individually with a fully irregular solution following the approach for χ_2 discussed above.

F. Asymptotic behavior of exchange potential

In analogy to other variants of the OPM,[19,29,38] representation (67) of G_k allows for a detailed analysis of the OPM [Eqs. (52) and (53)] for large r. While the extended form of Γ_k [Eq. (73)] complicates the discussion, the asymptotic behavior of the regular and irregular solutions given in Sec. II E provides all necessary information to follow the line of arguments sketched in Appendix B of Ref. 29. As the discussion is somewhat lengthy, it is relegated to the Appendix.

In the leading order the analysis leads to a Krieger-Li-Iafrate-type identity[38] for the exact exchange of RSDFT,

$$2\sum_{\sigma=\pm} \int_0^{\infty} dr \varphi^{\dagger}(r) P_{\sigma} \varphi(r) v_{\mathrm{x},\sigma}(r) = \int_0^{\infty} dr \varphi^{\dagger}(r) \frac{\delta E_{\mathrm{x}}}{\delta \varphi(r)}. \tag{91}$$

The next to leading order then determines the asymptotic behavior of $v_{\mathrm{x},\sigma}$ for finite systems,

$$v_{\mathrm{x},\sigma}(r \to \infty) = -\frac{1}{r}. \tag{92}$$

As in the nonrelativistic and in the spin-saturated limit, this behavior leads to a Rydberg series of unoccupied KS states, unlike the exponential decay of the LDA or GGA potential.

III. RESULTS

Neutral atoms have been extensively studied in the framework of RSDFT on the basis of the LDA and GGA.[16,17,49,53]

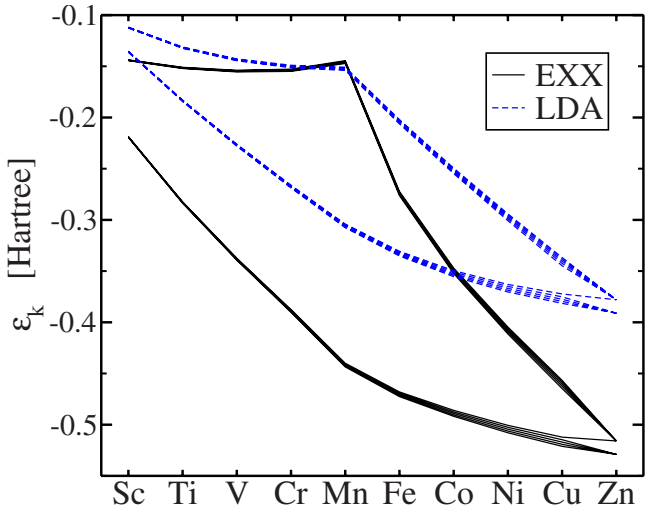

FIG. 1. (Color online) KS eigenvalues of $3d$ subshell for $3d$ elements with occupation $3d^n4s^2$: exact x-only results (EXX) versus LDA (Ref. 55) results.

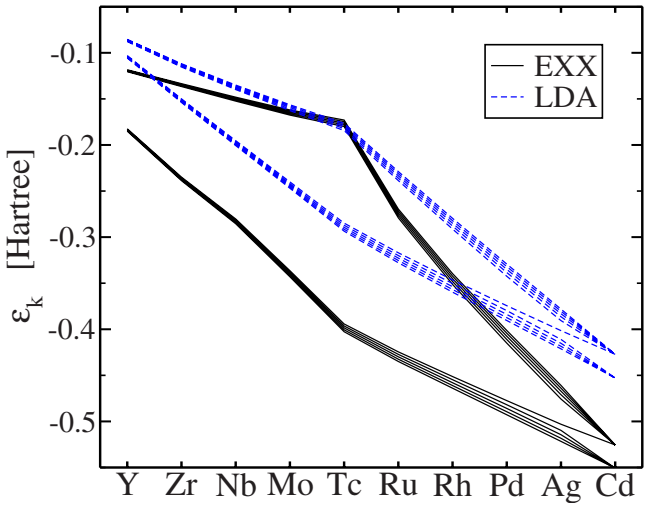

FIG. 2. (Color online) Same as in Fig. 1 for $4d$ elements with occupation $4d^n5s^2$.

The question for the role of the exact exchange in the case of atoms thus arises automatically. First atomic results obtained by self-consistent calculations with the exact exchange (EXX) have been presented in I, focusing on the relativistic corrections to the xc magnetic field. In the following we address three further topics, the relative importance of exchange splitting and spin-orbit coupling for the KS states, atomic hyperfine constants, and the *s*-*d*-transfer energies of the transition-metal elements.

All calculations have been done using finite difference methods, which imply a discretization of the OPM integral equations on the radial grid in analogy to Ref. 19. Large logarithmic meshes (up to 1600 grid points) have been combined with the Bulirsch-Stoer algorithm (see, e.g., Ref. 54) for the solution of Eqs. (28) and (55).

A. Spin-orbit coupling versus exchange splitting

The first obvious question addresses the relative importance of exchange versus spin-orbit effects. As the exact exchange yields more pronounced exchange splittings, i.e., favors spin polarization more than the LDA, one could expect the KS eigenenergies to reflect this increased importance of polarization compared to that of spin-orbit coupling. Figures 1–3 confirm this expectation.

Figure 1 shows the KS eigenvalues of the $3d$ subshell for the $3d$-transition-metal atoms, obtained for the lowest energy state with the configuration $3d^n4s^2$ for all of them. It is obvious that (i) for given σ all $m\sigma$ substates are essentially degenerate, (ii) occupied states are stabilized substantially by use of the exact E_x (with the stabilization being particularly pronounced for the first half of the subshell), and (iii) the ordering of the states follows closely Hund's first rule rather than the splitting expected from spin-orbit coupling. The only exception is Zn for which finally all $3d$ substates are occupied.

When comparing these results with those for the $4d$ subshell of the $4d$ elements (given in Fig. 2), one observes a broadening of the energies of the $m\sigma$ substates with the same polarization. The ordering according to spin, however, remains essentially intact, although the state $m=-\frac{5}{2}$ splits from the other majority-spin states somewhat earlier. This latter effect is even more pronounced for the $5d$ eigenvalues of the $5d$ atoms, plotted in Fig. 3. In the case of the LDA spin-orbit coupling now dominates the energetic ordering for the second half of the subshell. On the other hand, if the exact exchange is used, a substantial deviation of the $-\frac{5}{2}$ eigenvalue from those of the remaining majority-spin states is only observed for Au (and, of course, Hg). The differences between LDA and exact exchange are most obvious for the $6p$ series shown in Fig. 4.

In fact, for Pb the LDA essentially predicts a ground state with good j. The corresponding magnetic moment vanishes, so that the LDA does not reproduce the experimental $^3P_0$ ground state. The exact exchange, on the other hand, favors alignment of spins much more, so that the resulting energy gain can compete with the energy gain originating from cou-

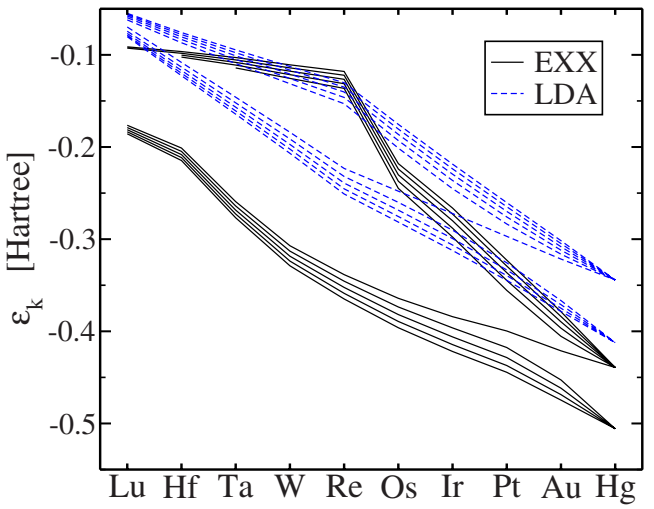

FIG. 3. (Color online) Same as in Fig. 1 for $5d$ elements with occupation $5d^n6s^2$.

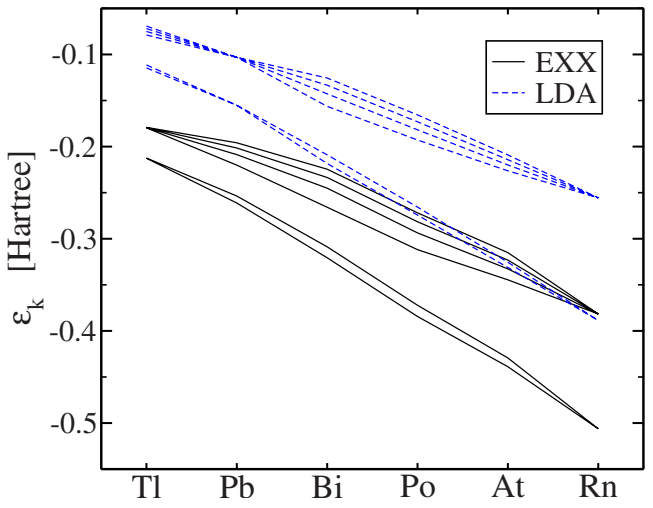

FIG. 4. (Color online) Same as in Fig. 1 for $6p$ elements with occupation $6p^n$.

pling of spin and orbital angular momentum to good j. As a consequence, the exact exchange leads to a ground state with magnetic moment $2.035\mu_B$, i.e., essentially two aligned spins as observed in experiment. Some reference data obtained with the exact exchange in RSDFT are listed in Table I.

B. Hyperfine constants

Using the algebra of irreducible tensor operators,[50] the hyperfine coupling between the magnetic moment of the nucleus and the magnetic field generated by the electrons at the position of the nucleus (the origin) can be expressed as

$$\hat{H}_{\mathrm{HF}} = -\gamma_I \frac{\langle n,J,J_z|\hat{B}_z|n,J,J_z\rangle}{J_z}\hat{\boldsymbol{I}}\cdot\hat{\boldsymbol{J}}, \tag{93}$$

where $\hat{\boldsymbol{I}}$ and $\hat{\boldsymbol{J}}$ denote the total angular-momentum operators of the nucleus and the electrons, respectively, γ_I is the gyromagnetic ratio of the nucleus,

TABLE I. Total energy E, exchange energy E_{x}, eigenvalue of highest occupied KS orbital ϵ_{HOMO}, and total magnetic moment $M=\int d^3r m_z(\boldsymbol{r})$ of some prototype open-shell atoms. A point nucleus is assumed ($c=137.035\,989\,5$ a.u., all energies in hartree, M in μ_B).

			HOMO				
Atom	$-E$	$-E_{\mathrm{x}}$	nl	m	σ	$-\epsilon_{\mathrm{HOMO}}$	M
Al	242.3277	18.1010	$3p$	$+\frac{1}{2}$	+	0.2093	1.000
Fe	1271.5436	54.7684	$4s$	$+\frac{1}{2}$		0.2446	3.998
Eu	10 847.6694	238.9380	$6s$	$+\frac{1}{2}$		0.1769	6.990
Os	17 274.2850	333.4783	$5d$	$-\frac{3}{2}$	–	0.2450	3.927
Au	19 039.8067	357.3234	$6s$	$-\frac{1}{2}$		0.2957	0.997

$$\gamma_I = \frac{\langle m,I,I|\hat{\mu}_z|m,I,I\rangle}{I}, \tag{94}$$

and both the nucleus and the electrons are assumed to be in states with good total angular momentum and z projection, $|m,I,I_z\rangle$ and $|n,J,J_z\rangle$, respectively. The hyperfine coupling constant a,

$$\hat{H}_{\mathrm{HF}} = a\hat{\boldsymbol{I}}\cdot\hat{\boldsymbol{J}}, \tag{95}$$

is thus given by

$$a = -\gamma_I \frac{\langle n,J,J_z|\hat{B}_z|n,J,J_z\rangle}{J_z}. \tag{96}$$

However, the magnetic field produced by the electrons is determined by the static electronic current $\boldsymbol{j}$ via the law of Biot and Savart,

$$\boldsymbol{B}_{\mathrm{HF}}(\boldsymbol{r}) = \langle n,J,J_z|\hat{\boldsymbol{B}}(\boldsymbol{r})|n,J,J_z\rangle = \frac{e}{c}\int d^3r'\boldsymbol{j}(\boldsymbol{r}')\times\frac{(\boldsymbol{r}-\boldsymbol{r}')}{|\boldsymbol{r}-\boldsymbol{r}'|^3}. \tag{97}$$

As the current is one of the basic variables of relativistic DFT, the field $\boldsymbol{B}_{\mathrm{HF}}$ generated by the ground state is a quantity which can be rigorously evaluated within DFT. Insertion of the relativistic KS current into Eq. (97) leads to

$$\boldsymbol{B}_{\mathrm{HF}}(0) = e\sum_k \Theta_k \int d^3r \phi_k^\dagger(\boldsymbol{r})\frac{\boldsymbol{r}\times\boldsymbol{\alpha}}{r^3}\phi_k(\boldsymbol{r}). \tag{98}$$

Using the form of the atomic KS spinors of RSDFT [Eqs. (25) and (26)], one can evaluate the angular integrations in Eq. (98) to obtain

$$\boldsymbol{B}_{\mathrm{HF}}(\boldsymbol{0}) = (0,0,B_{\mathrm{HF}}), \tag{99}$$

$$\begin{aligned} B_{\mathrm{HF}} = e\int_0^\infty dr\frac{1}{r^2}\sum_{nlm\sigma}\Theta_{nlm\sigma} \\ \times\Bigg\{-\frac{8m(l+1)}{(2l+1)(2l+3)}a^+_{nlm\sigma}(r)b^+_{nlm\sigma}(r) \\ +\frac{8ml}{(2l+1)(2l-1)}a^-_{nlm\sigma}(r)b^-_{nlm\sigma}(r) \\ -C_{lm}\begin{bmatrix} a^+_{nlm\sigma}(r)b^-_{nlm\sigma}(r) \\ +a^-_{nlm\sigma}(r)b^+_{nlm\sigma}(r)\end{bmatrix}\Bigg\}. \end{aligned} \tag{100}$$

Figures 5–8 show some prototype results for the hyperfine constant a obtained with the exact exchange in the framework of RSDFT. For the evaluation of hyperfine field (100) the KS ground state, i.e., the occupation of the m levels which gives minimum total energy, has been used. It turns out that for all atoms considered here the absolute value of

$$J_z = \sum_{nlm\sigma}\Theta_{nlm\sigma}m$$

associated with this state agrees with the total J of the true ground state. Similarly, the absolute value of the (noninteger) magnetic moment of the KS ground state,

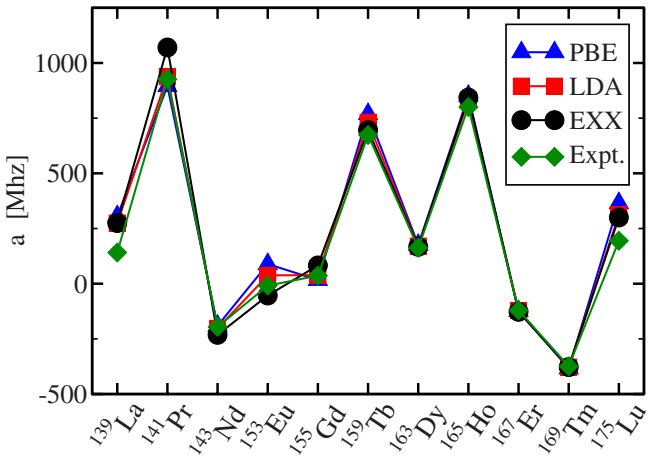

FIG. 5. (Color online) Hyperfine constants a for lanthanide elements: exact x-only (EXX), LDA,[55] and PBE-GGA (Ref. 57) results versus experimental data. Lines are only drawn to guide the eyes.

$$M_z = \int d^3 r m_z(\boldsymbol{r}),$$

is always very close to the total spin of the true ground state.

For the nuclei the most prominent isotope with nonvanishing a has been chosen. In order to account for the finite size of the nuclei, a Fermi charge distribution[56] has been applied for the evaluation of v_{ext}. The resulting corrections, however, are generally small compared to typical deviations of RSDFT results from experimental data.

In Fig. 5 the hyperfine constants of the lanthanide series are plotted, including numbers obtained with the LDA and the Perdew-Burke-Ernzerhof (PBE)-GGA.[57] It is immediately obvious that the RSDFT results follow the experimental trend throughout the $4f$ subshell quite closely. The largest deviations are observed for the lightest elements, ^{139}La and ^{141}Pr, as well as for the heaviest atom shown, ^{175}Lu. While for ^{139}La and ^{175}Lu all functionals give similar errors (with the GGA being somewhat less accurate than LDA and EXX), the exact exchange overestimates the experimental a clearly more than the LDA or GGA in the case of ^{141}Pr. On the other hand, for ^{153}Eu and ^{159}Tb the exact exchange is significantly closer to the experimental values than the conventional xc functionals.

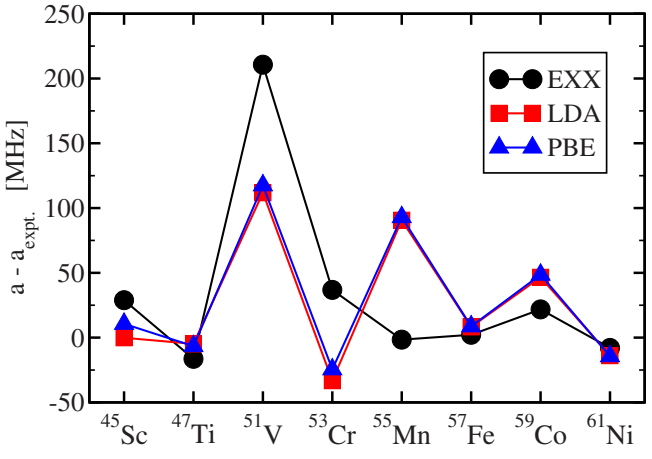

FIG. 6. (Color online) Deviation of hyperfine constants a from experimental value a_{expt}: exact x-only results (EXX) versus LDA (Ref. 55) and PBE-GGA (Ref. 57) data for $3d$-transition-metal elements.

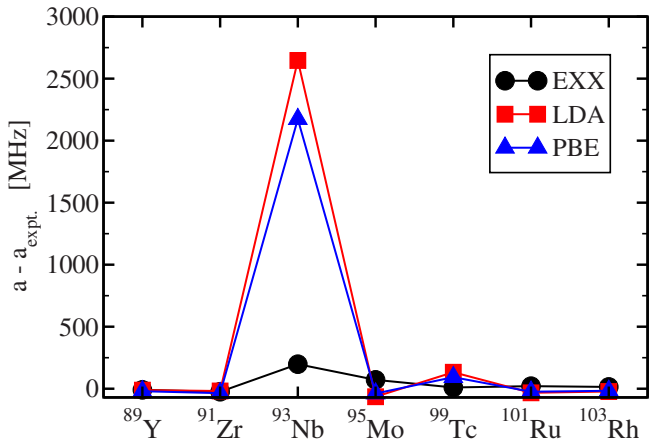

FIG. 7. (Color online) As in Fig. 6 for $4d$-transition-metal elements.

Figures 6–8 complement these results by providing the deviation of the RSDFT predictions for a from experiment for the transition-metal elements (the trends throughout the d shells are again well reproduced). For most elements the exact exchange leads to better agreement with the experimental a than the conventional xc functionals, the improvement being particularly obvious for the $4d$ series. However, there is also one noticeable exception, ^{51}V. This clearly points at the importance of correlation and orbital polarization for B_{HF}.

C. *s-d* transfer energies of transition-metal elements

The description of the transfer of an electron from an atomic s to a d orbital is a long-standing problem of DFT.[58–62] The relative stability of the two configurations involved is determined by the s-d-transfer energy ΔE, which,

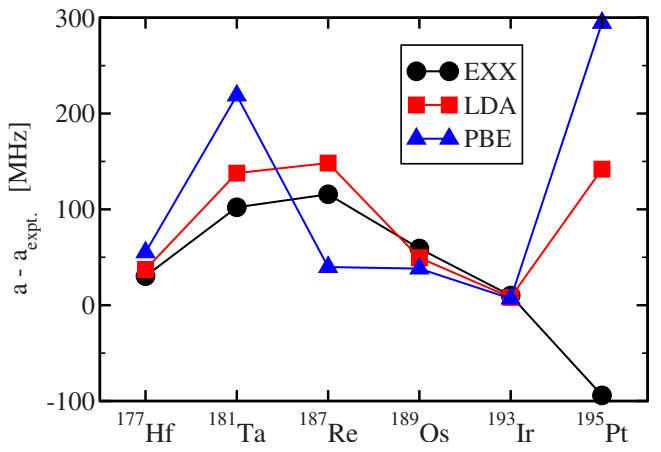

FIG. 8. (Color online) As in Fig. 6 for $5d$-transition-metal elements.

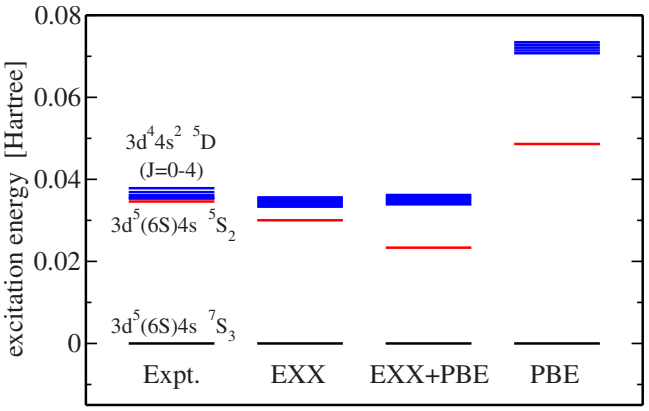

FIG. 9. (Color online) Low-lying levels of chromium atom: exact x-only results (EXX) versus data obtained from exact exchange plus PBE-GGA (Ref. 57) for correlation (EXX+PBE) as well as complete PBE-GGA and experimental numbers (Ref. 63). The experimental $3d^5(6S)4s\ ^5S_2$ state is only 0.7 mhartree lower than the lowest state ($J=0$) of the $3d^44s^2\ ^5D$ multiplet and can therefore not be resolved on the present scale.

in the case of the $3d$-transition-metal elements considered here, is given by

$$\Delta E = E[\text{core}, 4s^1 3d^n] - E[\text{core}, 4s^2 3d^{n-1}].$$

The LDA overestimates the stability of the $4s^13d^n$ configuration by typically 1 eV. On the other hand, it has been demonstrated that the combination of total relativistic Hartree-Fock energies with DFT correlation energies leads to much better results.[61] This immediately raises the question on how the exact exchange of RSDFT performs.

In order to set the stage we first consider the lowest-lying states of neutral chromium. The experimental excitation energies from the $3d^5(6S)4s\ ^7S_3$ ground state to the first-excited state $3d^5(6S)4s\ ^5S_2$ and to the multiplet $3d^44s^2\ ^5D$ are shown in Fig. 9.

Due to their differing symmetries all three levels are basically accessible to DFT, the $3d^5(6S)4s\ ^5S$ involving the inversion of the $4s$ spin and the $3d^44s^2\ ^5D$ level the s-d transfer process. As the total angular momentum J is not a good quantum number within the present RSDFT approach, the individual multiplet states of the $3d^44s^2\ ^5D$ level (with values of J between 0 and 4) cannot be resolved rigorously. Rather RSDFT provides states with given $|J_z|$ between 0 and 4, depending on the occupation of the $m\sigma$ substates available for the $3d$ level. These J_z-dependent KS states may be considered as resulting from the various multiplet states. In particular, the state with maximum $|J_z|=4$ can only be associated with $J=4$, thus providing rather unambiguous access to one of the multiplet states. Moreover, as the KS states for different J_z are not degenerate (see below), one is tempted to identify the single determinant KS state with $|J_z|=J$ as the KS representation of the multiplet state with total angular momentum J. In any case, the range of energies obtained for these KS states can be understood as a measure of the experimental multiplet splitting. The total energies resulting from application of the exact exchange to all possible ways to occupy the $m\sigma$ substates by four electrons with the same spin are listed in Table II.

TABLE II. Total energies E of all nonequivalent ways to generate the $3d^44s^2\ ^5D$ configuration of Cr via occupation of different $m\sigma$ substates with the same sign of the magnetization. All substates with $\sigma=-$ and the substate with $m=\frac{5}{2}$ remain unoccupied (all energies in hartree).

Occupation						
$m,\sigma=+$				m		
$\frac{3}{2}$	$\frac{1}{2}$	$-\frac{1}{2}$	$-\frac{3}{2}$	$-\frac{5}{2}$	J_z	$-E$ (hartree)
1	1	1	1	0	0	1049.7675
1	1	1	0	1	−1	1049.7669
1	1	0	1	1	−2	1049.7664
1	0	1	1	1	−3	1049.7658
0	1	1	1	1	−4	1049.7652

The energetic ordering of the states with respect to J_z is exactly the same as that of the experimental energies with respect to J, corroborating the identification of states indicated above. Similarly, the spread of the total energies of about 2 mhartree is close to the experimental multiplet splitting. In addition, the spread is much smaller than the differences between the $3d^44s^2$ energies and the ground-state energy of −1049.8009 hartree.

The range of excitation energies covered by the various occupations is indicated in Fig. 9, together with the EXX excitation energy to the $3d^5(6S)4s\ ^5S$ state. The EXX values turn out to be surprisingly close to their experimental counterparts, unlike the GGA excitation energies—the first-principles PBE-GGA shows the same type of deviation as the LDA.

In fact, the EXX excitation energies are so close to the correct values that one might wonder whether the agreement still persists after inclusion of correlation. As Fig. 9 demonstrates, this is not the case if GGA correlation is added to the exact exchange. However, it is well known that the quality of LDA and, to some extent, also GGA results is due to error cancellation between exchange and correlation and that therefore the combination of the exact exchange with LDA or GGA correlation does not give convincing results.[18]

For this reason one has to resort to an equivalent orbital-dependent representation of E_c at this point. So far, two types of first-principles orbital-dependent correlation functionals have been discussed in the literature, perturbation theory on KS basis[64–67] and the RPA as the simplest resummation of the KS perturbation series.[31,42,43,68] In view of the open subshell nature of the states involved only the latter functional can be used for the discussion of the s-d transfer. The RPA can be expressed as

$$E_c^{\text{RPA}} = \frac{1}{2}\int_0^\infty \frac{d\omega}{\pi}\{\ln|\det[\underline{\underline{1}} - \underline{\underline{S}}(i\omega)]| + \text{Tr}\,\underline{\underline{S}}(i\omega)\}, \quad (101)$$

where

TABLE III. Low-lying states of Cr: RPA+ correlation and resulting RSDFT total energies $E^{\mathrm{EXX+RPA+}}=E^{\mathrm{EXX}}+E_c^{\mathrm{RPA+}}$ for various occupations of the m_l substates of the $3d\uparrow$ level (all energies in hartree).

	Occupation of $3d\uparrow;m_l$								
Configuration	2	1	0	−1	−2	L_z	J_z	$-E_c^{\mathrm{RPA+}}$	$-E^{\mathrm{EXX+RPA+}}$
$3d^5\uparrow;4s^1\uparrow$	1	1	1	1	1	0	3	0.6108	1050.4117
$3d^5\uparrow;4s^1\downarrow$	1	1	1	1	1	0	2	0.6005	1050.3713
$3d^4\uparrow;4s^2$	1	1	1	1	0	2	0	0.5959	1050.3634
$3d^4\uparrow;4s^2$	1	1	1	0	1	1	1	0.5890	1050.3559
$3d^4\uparrow;4s^2$	1	1	0	1	1	0	2	0.5857	1050.3521
$3d^4\uparrow;4s^2$	1	0	1	1	1	1	3	0.5890	1050.3548
$3d^4\uparrow;4s^2$	0	1	1	1	1	2	4	0.5959	1050.3611

$$S_{ik,jl}(i\omega)=(kj\|il)C_{jl}(i\omega), \tag{102}$$

$$C_{kl}(i\omega)=\Theta_k(1-\Theta_l)\frac{2(\epsilon_k-\epsilon_l)}{\omega^2+(\epsilon_k-\epsilon_l)^2}, \tag{103}$$

where $(ij\|kl)$ is given by Eq. (11) and the trace runs over the multi-index ik of the matrix $\underline{\underline{S}}$.

As it stands, E_c^{RPA} is not particularly useful for the discussion of finite systems as atoms and molecules, as for these systems the second-order exchange (SOX) contributions are sizable. In order to account for these short-range contributions not included in the RPA, E_c^{RPA} has been augmented by the simplest approximation for the SOX energy,[69,70]

$$E_{\mathrm{c}}^{\mathrm{RPA+}}=E_{\mathrm{c}}^{\mathrm{RPA}}+E_{\mathrm{c}}^{\mathrm{LDA}}-E_{\mathrm{c}}^{\mathrm{LDA-RPA}}, \tag{104}$$

where $E_c^{\mathrm{LDA-RPA}}$ denotes the LDA for E_c^{RPA}. $E_c^{\mathrm{RPA+}}$ has been shown to give rather accurate correlation energies for atoms.[71]

In the present study $E_c^{\mathrm{RPA+}}$ has been evaluated perturbatively on the basis of nonrelativistic self-consistent EXX solutions—the nonadditivity of relativistic and correlation corrections is expected to be irrelevant for the $3d$ elements. In order to be consistent with the present atomic RSDFT solutions, a spherical average has been applied when evaluating the KS potential of the $3d^44s^2$ configuration. Only valence and semicore states are included in the evaluation of functional (104), i.e., all excitations of the K- and L-shell states are dropped in Eq. (101). The latter states are not expected to change much with the rearrangement of the occupation of the $3d$ and $4s$ states and only the energy difference associated with this rearrangement is of interest at this point. The RPA+ correlation energies obtained for the different configurations in case of the chromium atom are listed in Table III.

From the comparison of Tables II and III one, first of all, concludes that the correlation contribution to ΔE is only about half as large as the x-only value of ΔE. Moreover, the spread of $E_c^{\mathrm{RPA+}}$ among the various $3d^44s^2$ configurations is of the order of 10 mhartree and thus sizable. This makes the identification of the nonrelativistic, relativistic, and experimental states even more important. The nonrelativistic KS state with minimum energy has an empty $m_l=-2$ (majority-spin) substate, with the total orbital angular momentum L_z being antiparallel to the four aligned spins. This corresponds exactly to the RSDFT state with total $J_z=0$ and an empty $m=-\frac{5}{2}$ substate, which is the relativistic EXX state of minimum energy. The lowest energy EXX+RPA+ state of the $3d^44s^2$ configuration thus has $J_z=0$, consistent with the $J=0$ of the lowest experimental multiplet state. As the minimum-energy KS state, it is a KS representation of the lowest energy multiplet state. The corresponding EXX+RPA+ s-d-transfer energy is given by −48 mhartree, which has to be compared with the experimental value of −35 mhartree. In spite of the significant error of 13 mhartree this result represents clear progress over the GGA, which predicts a ΔE of −71 mhartree

There is one further RSDFT state for which a unique nonrelativistic counterpart can be identified: the state with maximum $|J_z|=4$ corresponds to the nonrelativistic state with $|L_z|=2$ and spin aligned with orbital angular momentum. This KS state can only be associated with the multiplet state with $J=4$. The s-d-transfer energies—EXX+RPA+: −51 mhartree; experiment: −38 mhartree—show the same deviation as observed for the minimum energies. This example demonstrates that the overall accuracy of EXX transfer energies is not particularly sensitive to the state chosen for the comparison with experiment.

Let us now consider the complete $3d$ series. In the case of the configuration $3d^n4s$ we focus on that multiplet for which the spins of the $3d$ electrons and that of the $4s$ electron are aligned. For all elements other than Cr and Cu this aligned-spin multiplet represents the first-excited level. It turns out that for each of the aligned-spin $3d^n4s$ configurations as well as for each of the $3d^n4s^2$ configurations of the complete $3d$ series the value of $|J_z|$ of the lowest energy RSDFT state is identical with the experimentally observed J value of the lowest energy multiplet state (as in the case of Cr discussed above). It is thus well justified to compare the RSDFT s-d-transfer energy between the two lowest energy states with the excitation energy between the two lowest multiplet states. In fact, this is also the most consistent approach in view of the basic philosophy behind DFT. Moreover, for the multiplets of Mn and all heavier atoms this J value agrees with the maximum J to which spin and orbital angular momentum can be coupled, so that the identification of states is unambiguous anyway. For Sc to Cr, on the other hand, the multiplet splittings of all states involved are below 2.5 mhar-

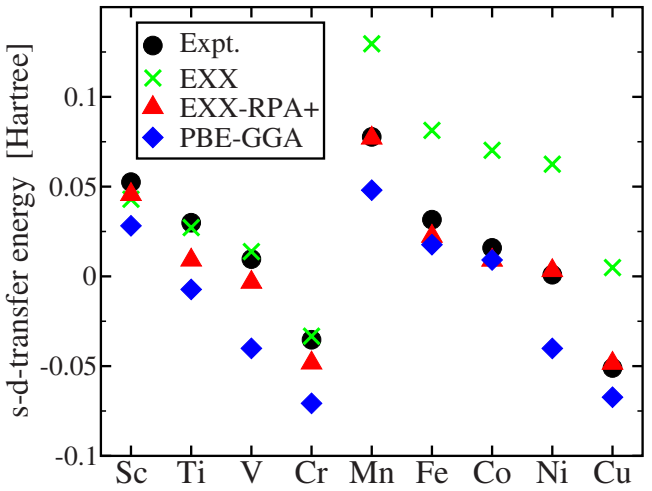

FIG. 10. (Color online) *s*-*d*-transfer energies of 3*d* elements: exact x-only results (EXX) versus data obtained from exact exchange plus RPA+ for correlation (EXX-RPA+), PBE-GGA (Ref. 57) and experimental numbers (Ref. 63) (RPA+=RPA+ second-order exchange within the LDA).

tree, so that a unique identification of states is not really necessary—the overall accuracy of the EXX+RPA+ approach is clearly lower than 2.5 mhartree. The result of this comparison is shown in Fig. 10, including EXX and PBE-GGA data.

It is obvious that the EXX scheme reproduces the changes in ΔE from one element to the next very well, with the exception of the transition from Cr to Mn, i.e., for half-filled *d* shell. The EXX *s*-*d*-transfer energies are extremely (fortuitously) close to the experimental ΔE for the first half of the shell but substantially off for the heavier elements. This offset vanishes as soon as RPA+ correlation is included. ΔE is now well reproduced throughout the shell. The agreement is particularly close for the second half of the shell, for which the identification of states is unambiguous. The most serious deviation of the EXX+RPA+ results is observed for Ti. Nevertheless, even in this case the EXX+RPA+ scheme predicts the correct ground-state configuration, unlike the PBE-GGA. Moreover, in the EXX+RPA+ approach the $3d^3 4s^2$ and $3d^4 4s^1$ configurations of V come out to be essentially degenerate, in contrast to the GGA which favors the $3d^4 4s^1$ configuration by 40 mhartree.

We have also examined the ΔE resulting from *s*-*d* transfer between the states with maximum *J*. The results, however, are almost indistinguishable from the values shown in Fig. 10 and therefore not plotted separately.

The EXX+RPA+ scheme thus represents clear progress compared to the GGA. The remaining error could be associated with (i) higher order correlation contributions not included in the RPA+, (ii) the LDA treatment of the SOX term, (iii) the nonrelativistic evaluation of the RPA+ energies, and (iv) the neglect of the paramagnetic current (i.e., of orbital polarization). The relative importance of these corrections remains to be investigated.

ACKNOWLEDGMENTS

Financial support by the Deutsche Forschungsgemeinschaft within the priority program 1145 (Grants No. EN 265/4-2 and No. EB 154/13-3) is gratefully acknowledged. The calculations for this work have been performed on the computer cluster of the Center for Scientific Computing of J.W. Goethe-Universität Frankfurt.

APPENDIX: ASYMPTOTIC BEHAVIOR OF EXCHANGE POTENTIAL: EXPLICIT PROOF

In this appendix we give an explicit derivation of identity (91) and the asymptotic behavior of v_x [Eq. (92)], following Appendix B of Ref. 29. We start by introducing a suitable notation. Dropping the index *k* for the state under consideration, utilizing Eq. (73), and defining

$$Y_0(r) = \varphi^\dagger(r)\varphi(r), \tag{A1}$$

$$Y_j(r) = \chi_j^\dagger(r)\varphi(r) \quad \text{for } j = 1,\ldots,4, \tag{A2}$$

$$Y_0^\pm(r) = \varphi^\dagger(r)P_\pm\varphi(r), \tag{A3}$$

$$Y_j^\pm(r) = \chi_j^\dagger(r)P_\pm\varphi(r) \quad \text{for } j = 1,\ldots,4, \tag{A4}$$

$$Y_{j+4}(r) = \int_r^\infty dr' Y_j(r') \quad \text{for } j = 1,3, \tag{A5}$$

$$Y_{j+4}(r) = \int_0^r dr' Y_j(r') \quad \text{for } j = 2,4, \tag{A6}$$

$$Y_9^\pm(r) = Y_1^\pm(r)Y_6(r) + Y_3^\pm(r)Y_8(r) + Y_2^\pm(r)Y_5(r) + Y_4^\pm(r)Y_7(r) - \frac{C}{2}Y_0^\pm(r), \tag{A7}$$

one can write the core ingredient of the response function as

$$\begin{aligned}\varphi^\dagger(r)P_\sigma G(r,r')P_{\sigma'}\varphi(r') = \Theta(r-r')[&Y_1^\sigma(r)Y_2^{\sigma'}(r') \\ &+ Y_3^\sigma(r)Y_4^{\sigma'}(r')] + \Theta(r'-r) \\ &\times[Y_2^\sigma(r)Y_1^{\sigma'}(r') + Y_4^\sigma(r)Y_3^{\sigma'}(r')] \\ &- Y_9^\sigma(r)Y_0^{\sigma'}(r') - Y_0^\sigma(r)Y_9^{\sigma'}(r').\end{aligned} \tag{A8}$$

Similarly, one can formulate the contribution of a single KS state to the right-hand side of the OPM equations as

$$\begin{aligned}\int_0^\infty dr'\varphi^\dagger(r)P_\pm G(r,r')\frac{\delta E_x}{\delta\varphi(r')} = &Y_1^\pm(r)X_6(r) + Y_3^\pm(r)X_8(r) \\ &+ Y_2^\pm(r)X_5(r) + Y_4^\pm(r)X_7(r) \\ &- Y_9^\pm(r)EX - Y_0^\pm(r)PX,\end{aligned} \tag{A9}$$

with

$$X_{j+4}(r) = \int_0^r dr'\chi_j^\dagger(r')\frac{\delta E_x}{\delta\varphi(r')} \quad \text{for } j = 2,4, \tag{A10}$$

$$X_{j+4}(r) = \int_r^\infty dr' \chi_j^\dagger(r') \frac{\delta E_x}{\delta\varphi(r')} \quad \text{for } j = 1,3, \tag{A11}$$

$$EX = \int_0^\infty dr' \varphi^\dagger(r') \frac{\delta E_x}{\delta\varphi(r')}, \tag{A12}$$

$$PX = \int_0^\infty dr' \left[\int_0^\infty dr'' \varphi^\dagger(r'') \Gamma(r'',r') - \frac{C}{2} \varphi^\dagger(r') \right] \frac{\delta E_x}{\delta\varphi(r')}. \tag{A13}$$

The asymptotic behavior of the $Y_j^{(\pm)}$ is obtained by combination of Eqs. (88)–(90) with Eqs. (82)–(85). For the elementary contractions and integrals one finds

$$Y_j(r\to\infty) = r^{2\alpha} e^{-2\beta r} Y_j^{(0)} \quad (j = 0,1,3), \tag{A14}$$

$$Y_j(r\to\infty) = Y_j^{(0)} \quad (j = 2,4), \tag{A15}$$

$$Y_j^\pm(r\to\infty) = r^{2\alpha} e^{-2\beta r} Y_j^{\pm(0)} \quad (j = 0,1,3), \tag{A16}$$

$$Y_j^\pm(r\to\infty) = Y_j^{\pm(0)} \quad (j = 2,4), \tag{A17}$$

$$Y_{j+4}(r\to\infty) = r^{2\alpha} e^{-2\beta r} \frac{Y_j^{(0)}}{2\beta} \quad (j = 1,3), \tag{A18}$$

$$Y_{j+4}(r\to\infty) = Y_j^{(0)} r \quad (j = 2,4), \tag{A19}$$

where the abbreviations

$$Y_j^{(0)} = \bar{\chi}_j^{(0)\dagger} \bar{\varphi}^{(0)}, \tag{A20}$$

$$Y_j^{\pm(0)} = \bar{\chi}_j^{(0)\dagger} P_\pm \bar{\varphi}^{(0)} \tag{A21}$$

have been introduced, with $\bar{\chi}_j^{(0)}$ denoting the four vectors resulting from Eqs. (82)–(85). Insertion into Eq. (A7) then gives

$$Y_9^\pm(r\to\infty) = r^{2\alpha} e^{-2\beta r} \left[(Y_1^{\pm(0)} Y_2^{(0)} + Y_3^{\pm(0)} Y_4^{(0)}) r + \frac{Y_2^{\pm(0)} Y_1^{(0)}}{2\beta} + \frac{Y_4^{\pm(0)} Y_3^{(0)}}{2\beta} - \frac{C}{2} Y_0^{\pm(0)} \right]. \tag{A22}$$

After insertion into the integral equation one can analyze the individual contributions in order to identify the leading term separately for each state k,

$$\int_0^\infty dr' \varphi^\dagger(r) P_\sigma G(r,r') P_{\sigma'} \varphi(r') v_{x,\sigma'}(r') = -r^{2\alpha+1} e^{-2\beta r} [Y_1^{\sigma(0)} Y_2^{(0)} + Y_3^{\sigma(0)} Y_4^{(0)}] \times \int_0^\infty dr' Y_0^{\sigma'}(r') v_{x,\sigma'}(r'), \tag{A23}$$

where it has been assumed that $v_{x,\sigma}(r)$ vanishes at least like $r^{-\epsilon}$ with $\epsilon > 0$. Equation (A25) neglects all terms which decay faster than $r^{2\alpha+1} e^{-2\beta r}$ by at least a fractional power of r. Similarly one obtains

$$\int_0^\infty dr' \varphi^\dagger(r) P_\sigma G(r,r') \frac{\delta E_x}{\delta\varphi(r')} = r^{2\alpha} e^{-2\beta r} Y_1^{\sigma(0)} X_6(r) + r^{2\alpha} e^{-2\beta r} Y_3^{\sigma(0)} X_8(r) + Y_2^{\sigma(0)} X_5(r) + Y_4^{\sigma(0)} X_7(r) - r^{2\alpha+1} e^{-2\beta r} [Y_1^{\sigma(0)} Y_2^{(0)} + Y_3^{\sigma(0)} Y_4^{(0)}] EX - r^{2\alpha} e^{-2\beta r} Y_0^{\sigma(0)} PX. \tag{A24}$$

The asymptotic behavior of $\delta E_x / \delta\varphi(r')$ is dominated by the exponential decay of the highest occupied orbital divided by the associated lowest multipole denominator r^{L+1}. The Fock-type integrals X_j thus have the asymptotic form,

$$X_{j+4}(r\to\infty) = r^{\alpha_h+\alpha-1} e^{-(\beta+\beta_h)r} X_{j+4}^{(0)} \quad \text{for } j = 1,3, \tag{A25}$$

$$X_{j+4}(r\to\infty) = \begin{cases} r^{\alpha_h-\alpha-1} e^{(\beta-\beta_h)r} X_{j+4}^{(0)} & \text{if } k \neq h \\ \ln(r) X_{j+4}^{(0)} & \text{otherwise} \end{cases} \quad \text{for } j = 2,4, \tag{A26}$$

where h denotes the highest occupied orbital. Note that for $k=h$ the monopole term of the self-interaction contribution, which is proportional to $1/r$, dominates the integrand in Eq. (A10). After insertion of Eqs. (A27) and (A28) into Eq. (A26) one can explicitly verify that only the highest occupied orbital is relevant in the OPM equations [Eqs. (52) and (53)] for large r,

$$0 = \int_0^\infty dr' \varphi^\dagger(r) P_\sigma G(r,r') \times \left\{ 2 \sum_{\sigma'=\pm} P_{\sigma'} \varphi(r') v_{x,\sigma'}(r') - \frac{\delta E_x}{\delta\varphi(r')} \right\} \tag{A27}$$

(we have dropped the index h for brevity—the subsequent discussion focuses on the highest occupied orbital only). Combining Eqs. (A25) and (A26) with Eq. (A29), analysis of the leading order leads to identity (91).

Let us now analyze the next important terms. To this aim we insert complete representations (A8) and (A9) into Eq. (A29) in order to include all potentially relevant terms,

$$\int_0^\infty dr' \varphi^\dagger(r) P_\sigma G(r,r') \left\{ 2 \sum_{\sigma'=\pm} P_{\sigma'} \varphi(r') v_{x,\sigma'}(r') - \frac{\delta E_{xc}}{\delta\varphi(r')} \right\} = Y_1^\sigma(r) \left[2 \sum_{\sigma'=\pm} \int_0^r dr' Y_2^{\sigma'}(r') v_{x,\sigma'}(r') - X_6(r) \right] + Y_3^\sigma(r) \left[2 \sum_{\sigma'=\pm} \int_0^r dr' Y_4^{\sigma'}(r') v_{x,\sigma'}(r') - X_8(r) \right] + Y_2^\sigma(r) \left[2 \sum_{\sigma'=\pm} \int_r^\infty dr' Y_1^{\sigma'}(r') v_{x,\sigma'}(r') - X_5(r) \right]$$

$$+ Y_4^\sigma(r)\left[2\sum_{\sigma'=\pm}\int_r^\infty dr' Y_3^{\sigma'}(r') v_{x,\sigma'}(r') - X_7(r)\right]$$
$$- Y_9^\sigma(r)\left[2\sum_{\sigma'=\pm}\int_0^\infty dr' Y_0^{\sigma'}(r') v_{x,\sigma'}(r') - EX\right]$$
$$- Y_0^\sigma(r)\left[2\sum_{\sigma'=\pm}\int_0^\infty dr' Y_9^{\sigma'}(r') v_{x,\sigma'}(r') - PX\right].$$

Once Eq. (91) is used, the terms proportional to $Y_1^\sigma(r)$ and $Y_3^\sigma(r)$ dominate asymptotically, as $X_6(r)$ and $X_8(r)$ diverge logarithmically for large r, according to Eq. (A28). Upon insertion of the asymptotically leading terms of $Y_1^\sigma(r)$ and $Y_3^\sigma(r)$ one thus has

$$0 = Y_1^{\sigma(0)}\left[2\sum_{\sigma'=\pm}\int_0^r dr' Y_2^{\sigma'}(r') v_{x,\sigma'}(r') - X_6(r)\right]$$
$$+ Y_3^{\sigma(0)}\left[2\sum_{\sigma'=\pm}\int_0^r dr' Y_4^{\sigma'}(r') v_{x,\sigma'}(r') - X_8(r)\right],$$

which allows for differentiation,

$$0 = Y_1^{\sigma(0)}\left[2\sum_{\sigma'=\pm} Y_2^{\sigma'}(r) v_{x,\sigma'}(r) - \chi_2^\dagger(r)\frac{\delta E_{xc}}{\delta\varphi(r)}\right]$$
$$+ Y_3^{\sigma(0)}\left[2\sum_{\sigma'=\pm} Y_4^{\sigma'}(r) v_{x,\sigma'}(r) - \chi_4^\dagger(r)\frac{\delta E_{xc}}{\delta\varphi(r)}\right].$$

As this relation has to be satisfied for both $\sigma=\pm$ one ends up with

$$2\sum_{\sigma'=\pm} Y_2^{\sigma'}(r) v_{x,\sigma'}(r) = \chi_2^\dagger(r)\frac{\delta E_{xc}}{\delta\varphi(r)} \equiv X_2(r), \quad \text{(A28)}$$

$$2\sum_{\sigma'=\pm} Y_4^{\sigma'}(r) v_{x,\sigma'}(r) = \chi_4^\dagger(r)\frac{\delta E_{xc}}{\delta\varphi(r)} \equiv X_4(r), \quad \text{(A29)}$$

and thus

$$v_{x,+}(r\to\infty) = \frac{1}{2}\frac{X_2(r)Y_4^-(r) - X_4(r)Y_2^-(r)}{Y_2^+(r)Y_4^-(r) - Y_2^-(r)Y_4^+(r)}, \quad \text{(A30)}$$

$$v_{x,-}(r\to\infty) = \frac{1}{2}\frac{Y_2^+(r)X_4(r) - Y_4^+(r)X_2(r)}{Y_2^+(r)Y_4^-(r) - Y_2^-(r)Y_4^+(r)}. \quad \text{(A31)}$$

Asymptotically, $X_2(r)$ and $X_4(r)$ are dominated by the monopole contribution to the self-interaction correction energy of the highest occupied orbital,

$$X_2(r\to\infty) = -\frac{2}{r}Y_2(r) = -\frac{2}{r}[Y_2^+(r) + Y_2^-(r)], \quad \text{(A32)}$$

$$X_4(r\to\infty) = -\frac{2}{r}Y_4(r) = -\frac{2}{r}[Y_4^+(r) + Y_4^-(r)]. \quad \text{(A33)}$$

Insertion into Eqs. (A32) and (A33) finally leads to Eq. (92).

[1] U. von Barth and L. Hedin, J. Phys. C **5**, 1629 (1972).
[2] G. Vignale and M. Rasolt, Phys. Rev. Lett. **59**, 2360 (1987).
[3] G. Vignale and M. Rasolt, Phys. Rev. B **37**, 10685 (1988).
[4] S. Pittalis, S. Kurth, N. Helbig, and E. K. Gross, Phys. Rev. A **74**, 062511 (2006).
[5] S. Rohra and A. Görling, Phys. Rev. Lett. **97**, 013005 (2006).
[6] S. Sharma, S. Pittalis, S. Kurth, S. Shallcross, J. K. Dewhurst, and E. K. U. Gross, Phys. Rev. B **76**, 100401(R) (2007).
[7] A. K. Rajagopal and J. Callaway, Phys. Rev. B **7**, 1912 (1973).
[8] E. Engel, in *Relativistic Electronic Structure Theory, Part 1. Fundamentals*, edited by P. Schwerdtfeger (Elsevier, Amsterdam, 2002), p. 524.
[9] A. H. MacDonald and S. H. Vosko, J. Phys. C **12**, 2977 (1979).
[10] H. Eschrig, G. Seifert, and P. Ziesche, Solid State Commun. **56**, 777 (1985).
[11] B. X. Xu, A. K. Rajagopal, and M. V. Ramana, J. Phys. C **17**, 1339 (1984).
[12] S. Doniach and C. Sommers, in *Valence Fluctuations in Solids*, edited by L. M. Falicov, W. Hanke, and M. B. Maple (North-Holland, Amsterdam, 1981), p. 349.
[13] P. Cortona, S. Doniach, and C. Sommers, Phys. Rev. A **31**, 2842 (1985).
[14] H. Ebert, J. Phys.: Condens. Matter **1**, 9111 (1989).
[15] L. Severin, M. Richter, and L. Steinbeck, Phys. Rev. B **55**, 9211 (1997).
[16] H. Yamagami, A. Mavromaras, and J. Kübler, J. Phys.: Condens. Matter **9**, 10881 (1997).
[17] E. Engel, T. Auth, and R. M. Dreizler, Phys. Rev. B **64**, 235126 (2001).
[18] E. Engel, in *A Primer in Density Functional Theory*, Lecture Notes in Physics Vol. 620, edited by C. Fiolhais, F. Nogeira, and M. Marques (Springer, Berlin, 2003), p. 56.
[19] J. D. Talman and W. F. Shadwick, Phys. Rev. A **14**, 36 (1976).
[20] Y. Li, J. B. Krieger, and G. J. Iafrate, Chem. Phys. Lett. **191**, 38 (1992).
[21] T. Kotani, Phys. Rev. B **50**, 14816 (1994).
[22] T. Kotani, Phys. Rev. Lett. **74**, 2989 (1995).
[23] T. Kotani and H. Akai, Phys. Rev. B **54**, 16502 (1996).
[24] M. Städele, J. A. Majewski, P. Vogl, and A. Görling, Phys. Rev. Lett. **79**, 2089 (1997).
[25] M. Städele, M. Moukara, J. A. Majewski, P. Vogl, and A. Görling, Phys. Rev. B **59**, 10031 (1999).
[26] A. Qteish, A. I. Al-Sharif, M. Fuchs, M. Scheffler, S. Boeck, and J. Neugebauer, Comput. Phys. Commun. **169**, 28 (2005).
[27] S. Rohra, E. Engel, and A. Görling, Phys. Rev. B **74**, 045119 (2006).

[28] S. Sharma, J. K. Dewhurst, and C. Ambrosch-Draxl, Phys. Rev. Lett. **95**, 136402 (2005).
[29] E. Engel, A. Facco Bonetti, S. Keller, I. Andrejkovics, and R. M. Dreizler, Phys. Rev. A **58**, 964 (1998).
[30] E. Engel, A. Höck, and R. M. Dreizler, Phys. Rev. A **61**, 032502 (2000).
[31] M. Fuchs and X. Gonze, Phys. Rev. B **65**, 235109 (2002).
[32] F. Furche and T. V. Voorhis, J. Chem. Phys. **122**, 164106 (2005).
[33] V. F. Lotrich, R. J. Bartlett, and I. Grabowski, Chem. Phys. Lett. **405**, 43 (2005).
[34] B. A. Shadwick, J. D. Talman, and M. R. Norman, Comput. Phys. Commun. **54**, 95 (1989).
[35] E. Engel, S. Keller, A. F. Bonetti, H. Müller, and R. M. Dreizler, Phys. Rev. A **52**, 2750 (1995).
[36] T. Kreibich, E. K. U. Gross, and E. Engel, Phys. Rev. A **57**, 138 (1998).
[37] D. Ködderitzsch, H. Ebert, and E. Engel, Phys. Rev. B **77**, 045101 (2008).
[38] J. B. Krieger, Y. Li, and G. J. Iafrate, Phys. Lett. A **146**, 256 (1990).
[39] D. Ködderitzsch, H. Ebert, H. Akai, and E. Engel, J. Phys.: Condens. Matter (to be published).
[40] S. Sharma, J. K. Dewhurst, C. Ambrosch-Draxl, S. Kurth, N. Helbig, S. Pittalis, S. Shallcross, L. Nordström, and E. K. U. Gross, Phys. Rev. Lett. **98**, 196405 (2007).
[41] S. Rohra, E. Engel, and A. Görling (unpublished).
[42] T. Kotani, J. Phys.: Condens. Matter **10**, 9241 (1998).
[43] F. Furche, Phys. Rev. B **64**, 195120 (2001).
[44] N. E. Dahlen and U. von Barth, J. Chem. Phys. **120**, 6826 (2004).
[45] E. Engel, H. Müller, C. Speicher, and R. M. Dreizler, in *Density Functional Theory*, edited by E. K. U. Gross and R. M. Dreizler, NATO Advanced Studies Institute, Series B: Physics (Plenum, New York, 1995), Vol. 337, p. 65.
[46] M. V. Ramana and A. K. Rajagopal, J. Phys. C **12**, L845 (1979).
[47] M. V. Ramana and A. K. Rajagopal, J. Phys. C **14**, 4291 (1981).
[48] E. Engel, S. Keller, and R. M. Dreizler, Phys. Rev. A **53**, 1367 (1996).
[49] H. Eschrig and V. D. P. Servedio, J. Comput. Chem. **20**, 23 (1999).
[50] M. E. Rose, *Elementary Theory of Angular Momentum* (Wiley, New York, 1957).
[51] J. C. Slater, *Quantum Theory of Molecules and Solids*, The Self-consistent Field for Molecules and Solids Vol. 4 (McGraw-Hill, New York, 1974), Appendix 3.
[52] W. Walter, *Gewöhnliche Differentialgleichungen: Eine Einführung* (Springer, Berlin, 2000).
[53] J. Forstreuter, L. Steinbeck, M. Richter, and H. Eschrig, Phys. Rev. B **55**, 9415 (1997).
[54] *Numerical Recipes*, edited by W. H. Press, B. P. Flannery, S. A. Teukolsky, and W. T. Vetterling (Cambridge University Press, Cambridge, 1989).
[55] S. H. Vosko, L. Wilk, and M. Nusair, Can. J. Phys. **58**, 1200 (1980).
[56] W. R. Johnson and G. Soff, At. Data Nucl. Data Tables **33**, 405 (1985).
[57] J. P. Perdew, K. Burke, and M. Ernzerhof, Phys. Rev. Lett. **77**, 3865 (1996).
[58] J. Harris and R. O. Jones, J. Chem. Phys. **68**, 3316 (1978).
[59] J. Harris and R. O. Jones, J. Chem. Phys. **70**, 830 (1979).
[60] O. Gunnarsson and R. O. Jones, Phys. Rev. B **31**, 7588 (1985).
[61] J. B. Lagowski and S. H. Vosko, Phys. Rev. A **39**, 4972 (1989).
[62] R. E. Watson, G. W. Fernando, M. Weinert, Y. J. Wang, and J. W. Davenport, Phys. Rev. B **43**, 1455 (1991).
[63] Y. Ralchenko, A. E. Kramida, J. Reader, and N. A. Team, NIST Atomic Spectra Database (Version 3.1.5), National Institute of Standards and Technology, Gaithersburg, MD, 2008 (http://physics.nist.gov/asd3).
[64] A. Görling and M. Levy, Phys. Rev. A **50**, 196 (1994).
[65] E. Engel and R. M. Dreizler, J. Comput. Chem. **20**, 31 (1999).
[66] S. Ivanov, S. Hirata, and R. J. Bartlett, J. Chem. Phys. **116**, 1269 (2002).
[67] H. Jiang and E. Engel, J. Chem. Phys. **125**, 184108 (2006).
[68] N. E. Dahlen and U. von Barth, Phys. Rev. B **69**, 195102 (2004).
[69] S. Kurth and J. P. Perdew, Phys. Rev. B **59**, 10461 (1999).
[70] Z. Yan, J. P. Perdew, and S. Kurth, Phys. Rev. B **61**, 16430 (2000).
[71] H. Jiang and E. Engel, J. Chem. Phys. **127**, 184108 (2007).